Structures 50 (2023) 538–560

Contents lists available at ScienceDirect

Structures

journal homepage: www.elsevier.com/locate/structures

Assessment of historic buildings after an earthquake using various advanced techniques

Gokhan Kilic *

Department of Civil Engineering, Izmir University of Economics, Izmir, Turkey

ARTICLE INFO

Keywords:
Historic Structure
GPR
Thermal Imaging
NDT
FTIR Spectroscopy

ABSTRACT

Monuments are structures with historical, archaeological, and cultural qualities. They were not designed or constructed to be earthquake resistant, and so pose risks to the community and are vulnerable to collapse or irreversible damage, particularly in seismically active areas. This study conducted a condition assessment of two different historic buildings to estimate their functional life following an earthquake on Samos Island on October 30, 2020. The study combined laboratory analysis, polarized optical microscope analysis, and FTIR (Fourier Transform Infrared Spectroscopy) spectral data analysis along with advanced techniques, such as Ground Penetrating Radar (GPR), thermal imaging, and Resistivity Measurement (RM). The signal and image analyses demonstrated the successful application of an integrated approach, with implications for protecting the constructed cultural heritage for a covering both scientific maintenance and decision making.

1. Introduction

Masonry structures in historic districts are vulnerable to seismic damage due to alterations over time and both the type and condition of construction elements. Updating systematic research on constructed heritage can provide a vast amount of data for identifying recursive features that may increase vulnerability and damage. The 2020 Samos Island earthquake in Greece struck with a magnitude of Mw 7.0, causing damage along the northern Samos coast and major localized damage in multi-story structures in Izmir, Turkey [1]. The first case study concerns a building that now functions as a mosque in Izmir's Urla district while the second concerns a Protestant church located in Izmir's Buca district (Fig. 1).

Earthquakes are cyclical but relatively rare natural occurrences that can significantly damage living habitats [2]. Turkey is situated on one of the world's most currently active seismic zones, namely, the Eastern Mediterranean. Western Turkey is particularly at risk because of the East Mediterranean subduction zone [3].

In the majority of studies on seismicity in Turkey, the features of historical earthquakes are often simply described, as reported in the national earthquake records. However, it is clear when evaluating nearby or distant earthquakes that additional factors should be considered, including as the local geology and tectonics, ground conditions, the seismic dynamics of the buildings, and the usage of earthquake-resistant construction materials. Since not all areas of Izmir city are equally stable, it is likely that past earthquakes that affected the whole of the city's settlements were caused by seismic sources passing through, or close to the city's core. The majority of the masonry buildings in the Izmir region are listed as historical landmarks. Turkey has several historic structures situated in an earthquake-prone areas that could sustain severe or significant damage in the event of any future earthquakes [4,5].

Determining the load-bearing capability of old masonry structures is a particularly challenging issue but an important step in protecting ancient structures from threats to their structural integrity. In countries like Turkey, an analysis of seismic risk is also a key part of the process. To make suitable maintenance judgements, a credible risk assessment for a historic structure presents various challenges, requiring both qualitative and quantitative approaches [6]. Qualitative data can be acquired through inspections of degradation, in combination with flaws, in combination with relevant literature searches. Quantitative data gathering, on the other hand, is far more complicated, expensive, and time-consuming requiring high levels of expertise, and should only be used if qualitative techniques fail to produce the necessary evidence [7].

Developed societies must preserve heritage buildings for future generations to consolidate a collective public memory that generates a sense of belonging via access to cultural assets. [8–10]. Heritage building conservation involves adequate structural protection,

* Corresponding author: Sakarya Cad. No:156, Balçova, 35330 Izmir, Turkey.
E-mail addresses: gokhan.kilic@ieu.edu.tr, gkilic@hotmail.co.uk.

https://doi.org/10.1016/j.istruc.2023.02.033
Received 31 October 2022; Received in revised form 18 January 2023; Accepted 6 February 2023
Available online 18 February 2023

appraisal, and monitoring to allow implementation of maintenance principles. Preservation includes historical, cultural, and engineering aspects, and necessitates a multidisciplinary and multicultural approach [7,11]. Historic buildings, such as mosques and churches, are important historical and cultural markers, and thus of interest to the general public. Unfortunately, these buildings may be weakened, and even collapse due to natural processes such as live load vibrations, which cause damage, including fractures. More specifically, major earthquakes and high wind loads can severely damage or even bring down tall and narrow structures such as the minarets of historic mosques and the towers of historic churches. These taller structures are particularly vulnerable to excessive tensile strains because mortar is generally the only element holding their masonry walls together [12–15].

Earthquakes produce additional loading through vibrations and building components are harmed by the arsing shear strains. Collapse frequently occurs because masonry, especially when under great compression stress, has poor resistance to bending and shear. The three main masonry failure modes are sliding shear failure, rocking, and diagonal cracking (Fig. 2) [16–18].

Non Destructive Testing (NDT) methods are extensively used because they can provide valuable information on a monument's current status and response with minimum invasion [19–22]. Each NDT method has its own strengths and limitations for historic structure diagnostics and monitoring. A complete methodology should therefore combine these methods to maximize the data about the building and its pathologies [23,24]. As established in different case studies [2,3], it is now common practice to combine NDT for analytical, conservation, and monitoring dedications, underlining these approaches as the primary instrument to detect defects before any restoration interventions, and subsequently, to monitor their effectiveness [26–29]. The process includes the use of many different NDT methods, such as laboratory analyses, polarized optical microscope studies, GPR, resistivity measurement, infrared thermography, and FTIR spectrometry. By comparing the findings from these different methods, researchers can develop a precise picture of the ancient building's structural health (Fig. 3).

The GPR and RM are two major geophysical methods applied to historic buildings to determine the causes of subsurface holes, the magnitude of deformations and fractures in the ground and building, geometric behaviour patterns, and soil-structure interface and modifications. GPR technology is commonly used to screen and monitor the health of historic buildings. 2D resistivity approaches can reveal moisture distributions inside old porous stonework, especially when combined with simulated driving rain [30–33]. Moisture is a well-known contributor to the degradation of porous stone, therefore, surveys are conducted before and after simulated rainfall to determine the effects of soaking and drying.

Historic mortars may contain a combination of aggregates, water, and binders, usually limestone, and unfortunately, their characterization is extremely challenging, and necessitates a lengthy laboratory experimentation program. There are numerous inherent variables, which may differ according to their location and age [34,35]. After a general assessment by visual inspection, laboratory analyses, and NDT procedures, a low magnification binocular lens was also used in this study for a more detailed analysis of dispersions or thin sections, using polarized microscopy.

Historical buildings and monuments degrade over time or may be severely damaged by natural disasters such as earthquakes. Studies on historical buildings have variously focused on the following; NDT methods, experimental studies in laboratories, visual inspection of

Fig. 1. Locations of the case studies and epicentre of Samos Island earthquake (October 30th, 2020). (a) Case Study 1; (b) Case Study 2.

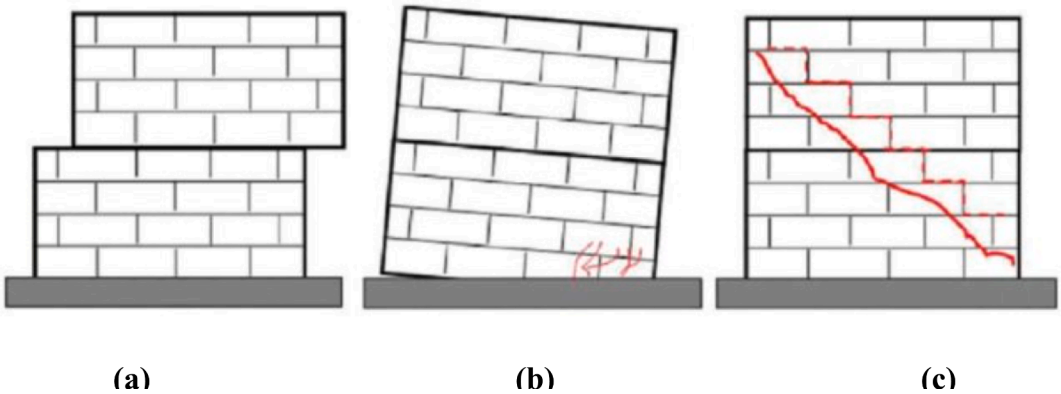

Fig. 2. Masonry wall in-plane failure types typically include: (a) sliding shear failure; (b) rocking; and (c) diagonal cracking [16].

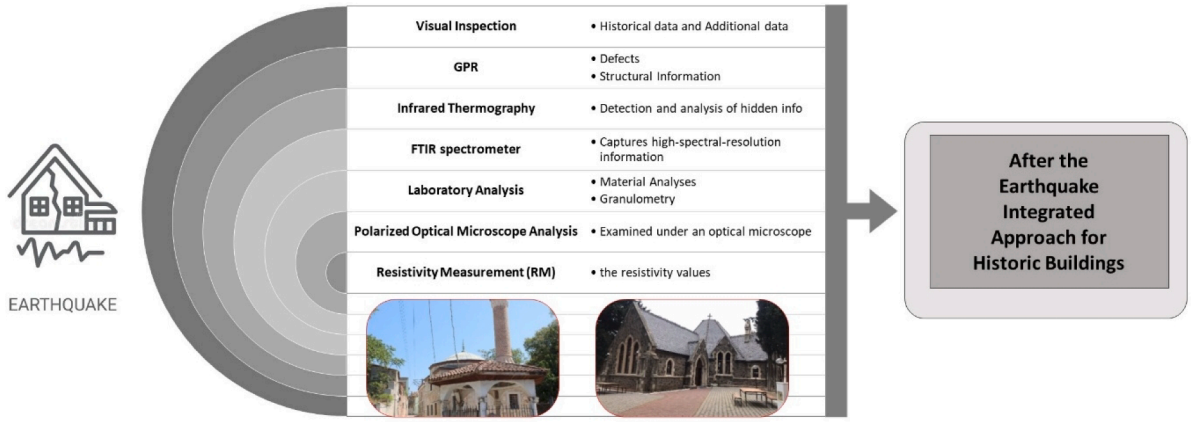

Fig. 3. Schematic depiction of the Integrated Approach for Historic Buildings after an Earthquake.

structural damage, monitoring of cracks, repairs and additions of the building, wall morphology, ground conditions, and architectural features. The information obtained with the finite element method determines the type of analysis is performed. The process of defining the structure is numerical modelling or mathematical modelling, which takes into account its geometric dimensions, the movement capabilities and degrees of freedom of the joints of the supports and structural system elements, and the loads acting on the structure,. In Fig. 4, the three-

Fig. 4. 3D drawing of the Case Studies.

dimensional images for the numerical models prepared to examine the earthquake resistance of the Case Study 1 and Case Study 2 respectively, are shown.

Modern industrial advances have increased the effectiveness of NDT methods in built cultural heritage preservation, making them key tools for characterizing materials, detecting wear and degradation, assessing intervention effectiveness, and evaluating compatible materials and processes [36,37]. In this study, an additional goal of the on-site examination was to assess the preservation condition of mosaics, determine the effects of earlier interventions, and reveal any hidden mosaics under the outward plastered surfaces.

The infrared spectra of absorption or emission of solids, liquids, or gases can be measured using an FTIR spectrometer, which gathers wide range of high-spectral-resolution information. Surface locations in catalysts can be assessed highly effectively using FTIR spectroscopy of probe molecules since each adsorbate's spectrum is distinct and highly reliant on the type of surface bonding to the local environment [38–40]. It is therefore essential to choose the most appropriate probe molecule because certain probes are likely to bind to particular locations. This makes identification and evaluation possible based on the absorption strength.

Integrated approaches have been emphasized for assessing and monitoring historic structures, including conventional methods locating flaws and deformities. However, additional laboratory examination is required for constructional improvements [27,41]. Because of the potential diversity and complexity of materials and structural systems in these constructions, it is essential to identify the processes and building materials employed. Using inappropriate materials for interventions can cause significant structural damage [42,43], therefore NDTs play critical role [44–47].

2. Historic buildings and Vısual Inspectıon

As previously stated, visual examination is an effective way to assess the condition of structures; as well as being cost-effective, it quickly detects visible flaws, including fractures, moisture penetration, and delamination [48]. However, it provides only limited information, and should be combined with other inspection techniques for a more comprehensive review. The two case studies here were subjected to extensive visual inspection, as detailed in the results section. However, visual inspection is generally only the first stage in a complete situation audit, followed by a more in-depth inquiry if necessary. By combining NDT testing and laboratory inspections, a full evaluation strategy collects both qualitative and quantitative data. These rather costly procedures, can be justified in terms of time-saving.

2.1. Case study 1- Izmir-Urla Haci Turan Kapan mosque

The first case study was the Izmir-Urla Haci Turan Kapan Mosque (Fig. 5), a historic Ottoman structure constructed in the mid-16th century and then extended on two sides in the 19th century [49]. The original central part was connected to the new sections via several arched corridors, built at various times before and after the extensions. The mosque has a square design with a single dome supported on an octagonal shaft and composed of cut stone and rubble stone. The sanctuary is illuminated by three rectangular windows at the lowest level and one on each side of the mosque-mihrab. The three-sectioned tiled narthex to the north has a minaret whose base extends as far as the dome pulley. The mosque courtyard was demolished to make way for a road and square, but the original fountain remains intact next to the road.

Each structural section of the building was visually assessed internally and externally, revealing that the material used were masonry, comprising brick, stone, and mortar. Among the defects discovered were degradation, water seepage, cover delamination, and large zones of cracking. Delamination-induced degradation was also discovered, necessitating repairs to the structure's west façade and the whole ceiling. One very large crack and other deformations can be seen in Fig. 6.

Fig. 5. Front View of case study 1 building.

2.2. Case study 2- Buca Protestant Baptist church

Buca Protestant Baptist Church was founded in 1834 as an independent Protestant Anglican church before being rededicated as a Baptist church. Its original structure was that of a small village church in the form of a chafel "chapel". It was renovated following an edict issued by Abdulaziz, the then Ottoman sultan, in 1865 [50] and used as a place of worship until 1961. In 1865, it was transferred to Buca Municipality and used as a wedding hall and cultural centre [51]. In 2001, an agreement was made to restore the building as a functioning church (Fig. 7).

The decorative stained glass in the church today is a replacement for the original, which was moved to Alsancak Church for protection following social unrest in 1964. A multi-purpose meeting building was built to the rear in 2004 [51]. The visual inspections did not reveal any significant cracks or deformations. Fig. 8 shows a few minor cracks and deformations.

3. Methodology

Extreme caution is required when using intervention techniques to preserve historical structures, including meticulous documentation of the structure's status. In the present study, a combination of laboratory analyses and ground-based NDT evaluation were used to develop a unique "integrated" holistic non-destructive technique for structural monitoring of historic structures. The first section reviews the condition of the two historic structures following an earthquake, explains key difficulties in terms of structural behaviour and functioning, and

Fig. 6. Case study 1: Serious crack inside the structure and other deformations.

Fig. 7. Front View of case study 2 building.

introduces the primary evaluation methodologies for identifying structural integrity-related issues. The additional methods used were visual examination, GPR, thermal imaging, and RM, as well as analyses carried out in a laboratory, using a polarized optical microscope, and FTIR. Due to the difficulty in determining the accuracy of tomographic pictures, ERT imaging has some limitations. In high conductivity materials like clay soils and salt-contaminated soils, the use of GPR is severely constrained. Understanding thermal pictures, especially for materials with erratic temperatures, is difficult, because changing emissivity and surface reflections make it difficult to get accurate temperature measurements. The combined results of these each approaches were used to then compared to create a highly accurate assessment of the historic building's structural condition following the earthquake (Fig. 9).

GPR is sensitive to changes in material composition, but to detect changes, it requires mobility. With surface-penetrating or ground-penetrating radar, fixed objects must be moved to allow the radar to analyse the targeted region by searching for variations in material composition. Resistivity measurement (RM) is limited in high-conductivity materials, such as clay soils and salt-contaminated soils. Thermal imaging has many limitations, including camera' difficulty in penetrating glass because thermal radiation may be reflected off shining surfaces, and challenges in interpreting images when items are subject to fluctuating temperatures.

Due to dynamic loadings, such as those caused by wind and earthquakes, reinforced concrete buildings require frequent, accurate, and dependable monitoring. In contrast, historical structures are cultural heritage assets, and these inherently provide limited opportunities for sampling or excavating portions for structural examination.

It is important to assess a historic building's state, particularly if damaged by a natural disaster, and even more so if there were pre-

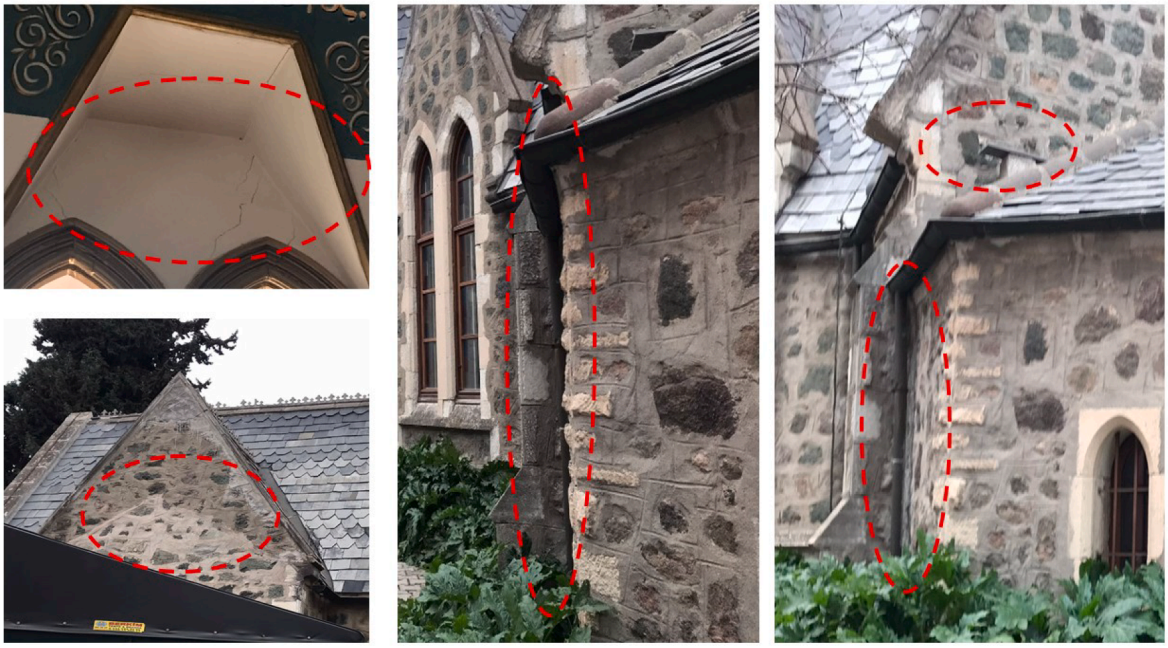

Fig. 8. Case study 2: Few minor cracks and deformations on internal and external walls.

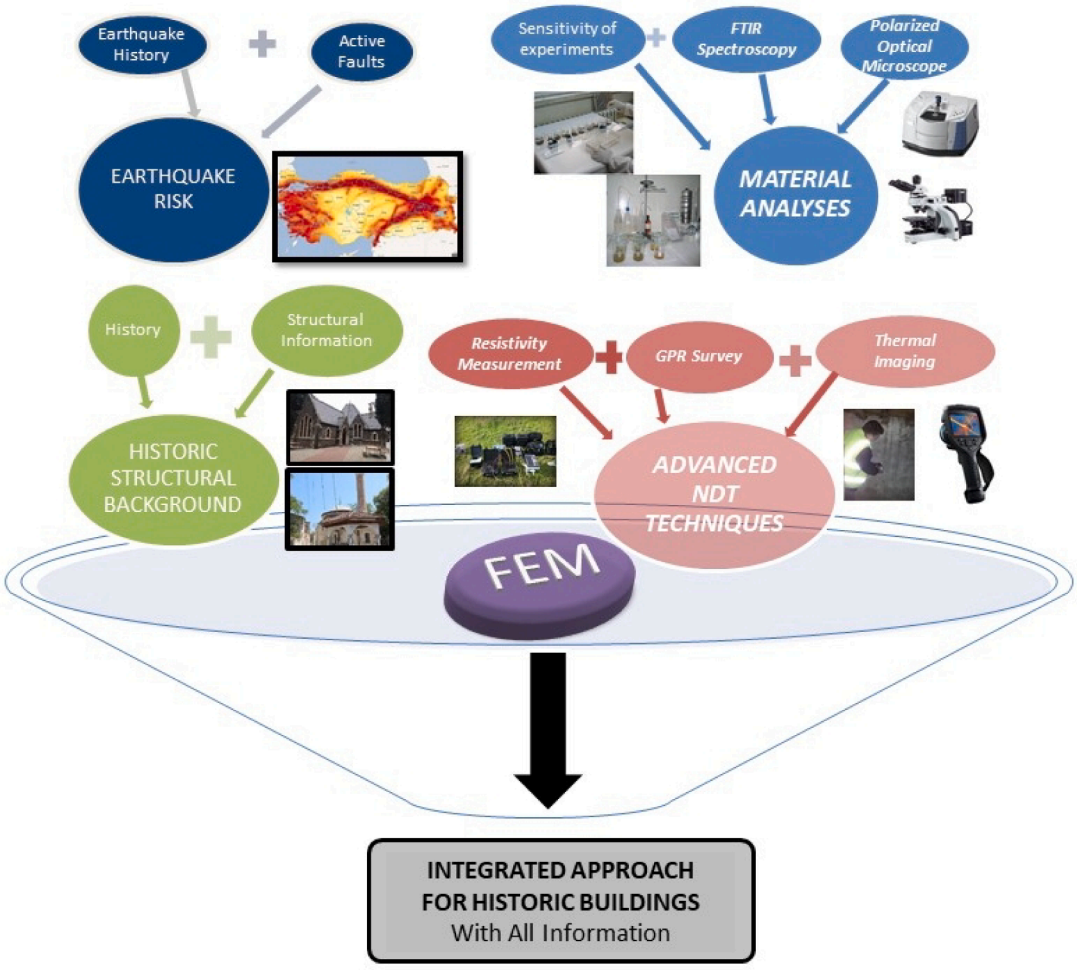

Fig. 9. Methodology for the Integrated Approach with all information.

existing issues. Thorough knowledge about the building's pre-existing state allows for appropriate risk assessment and the adoption of a suitable maintenance plan. The structure should be inspected as soon as possible after an earthquake to verify its safety state. Different methodologies are required for assessing pre-event and post-event safety situations; the former aims to determine the possible degree of risk whereas the latter determines the level of harm and any repairs required.

3.1. Laboratory material analysis

The main aim of this study was to document the building materials used in the two historical structures. Repairs had been undertaken in both buildings and their original structures were investigated. The following analyses, and methods were used to examine them:

- Spot salt-type tests (SO_4^{2-}, Cl^-, PO_4^{3-}, CO_3^{2-}, NO_3^-, NO_2^-)
- Physical tests (hardness, porosity, density, water absorption capacity)
- Conductometric analysis (total salt dissolved in water test)
- Acidic aggregate / binder analysis
- Granulometric analysis in aggregate (particle distribution in aggregate)
- Petrographic micromorphological thin/bright section optical microscope analysis

Fig. 10 presents the descriptions of the samples taken from different locations of the two historical buildings.

The size of the samples taken from two different historical buildings are presented in Fig. 11.

Analysis was conducted on stone/rock, mortar, plaster, and ceramic samples (Fig. 11) sampled during fieldwork on 16–17 July 2021. Descriptions of all samples taken from the historical buildings are given in Table 1.

3.1.1. Material analyses

The preliminary and process experiments were conducted either during sampling in the field or before the laboratory analyses to

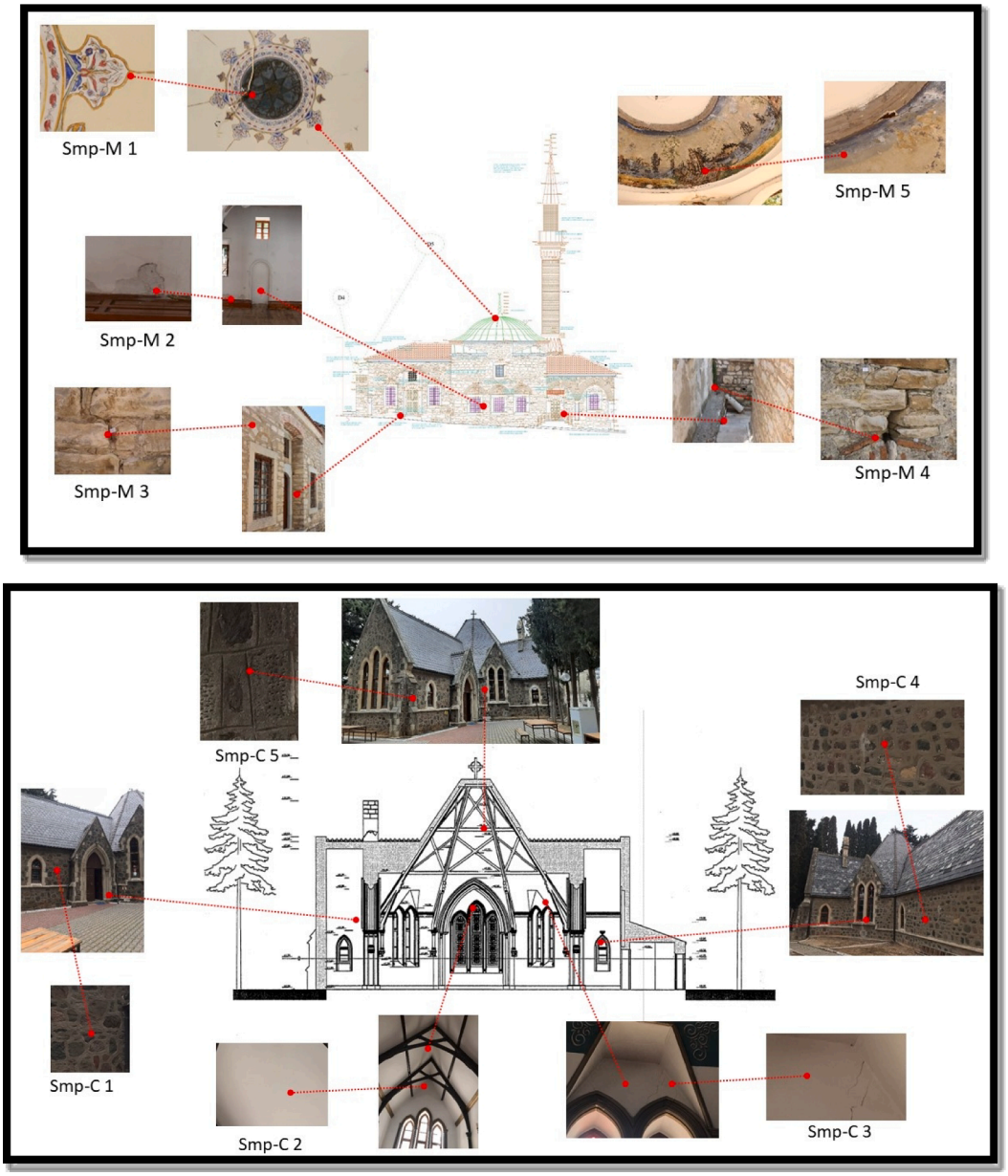

Fig. 10. Stone and rock samples used in the laboratory experiments, and their locations.

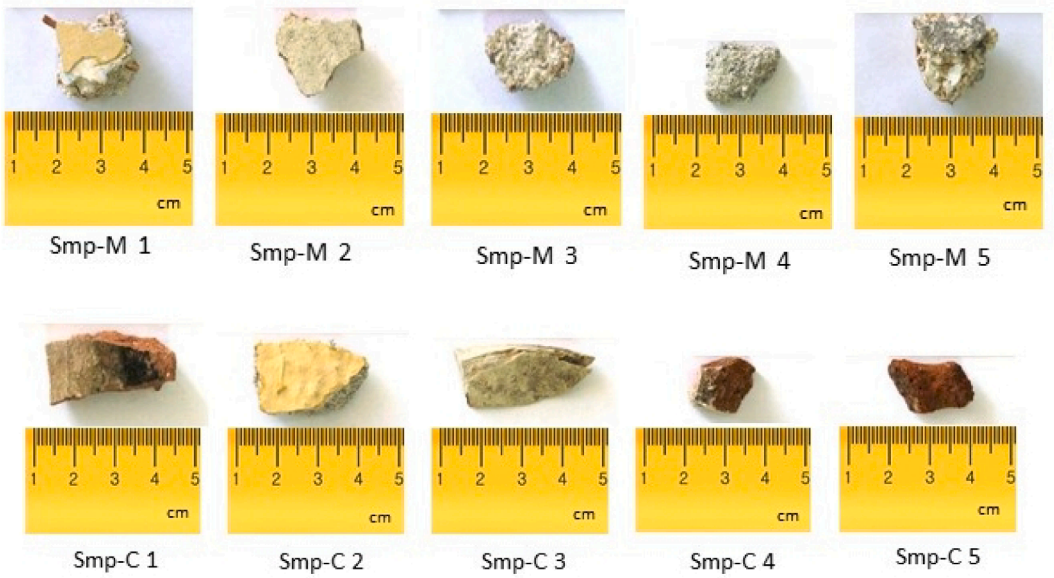

Fig. 11. Plaster, stone, rock, ceramic, mortar samples.

Table 1
Plaster, stone, rock, ceramic, mortar samples with descriptions.

Specimens	Descriptions
Smp- M 1	Plaster, Over the plant motif from the upper floor east wall
Smp- M 2	Plaster, repair plaster from east of north façade east window
Smp- M 3	Stone, West façade from the upper floor level near the roof
Smp- M 4	Stone, Lower floor entrance from the east wall trench 0.5 m from the floor
Smp- M 5	Plaster, Over the plant motif from the outside structure roof
Smp- C 1	Stone, West façade, near northwest corner at 2 m level
Smp- C 2	Plaster, Front façade from the level near the roof
Smp- C 3	Plaster, Over the plant motif from the upper floor east wall
Smp- C 4	Stone, West façade, near northwest corner at 2 m level
Smp- C 5	Mortar, Joint mortar from the opening in the north wall

determine the natural properties of the materials, and properties acquired due to environmental effects (rain, snow, day-night temperature differences, air pollution, exhaust gases, etc.). When examining a historical building's materials (soil, stone, ceramic, mortar, etc.), it is critical to determine the presence of any water-soluble salts on or in the body. These tests, which give quantitative values between specific volumetric limits, are generally used to determine the presence of the following salts: sodium, potassium and magnesium salts, sulphates, phosphates, nitrates and nitrites, chlorine and carbonate compounds, etc [25].

The following spot salt type experiments (SO_4^{2-}, Cl^-, PO_4^{3-}, CO_3^{2-}, NO_3^-, NO_2) were conducted on the stone and ceramic samples (Fig. 12):

- Sulphate experiments (SO_4^{2-}) are used for plasters and mortars, especially to identify gypsum-containing binders and the effects on the material of air pollution from flue gases (sulphation).
- Chlorine experiments (Cl^-) are used to show proximity to the effects of sewage (cleaning materials) from the interaction of cement-containing mortars with moisture and in places exposed to sea water.
- Phosphate experiments (PO_4^{3-}) reveal animal, plant, and food residues, found close to waste disposal/outdoor eating areas near or on the structures themselves, on the material's surface from sewage effects, or in the material content due water-based transport of soil content from the ground to the material. These can be detected at floor levels connected to the space, in plant-straw found in the top layer, or in mortars and plasters.
- Carbonate experiments (CO_3^{2-}) identify lime content in plasters and mortars.
- Nitrite (NO_2^-) and nitrate experiments (NO_3^-) detect the presence of these compounds in the black layers formed on the material in areas with intense traffic and air pollution.

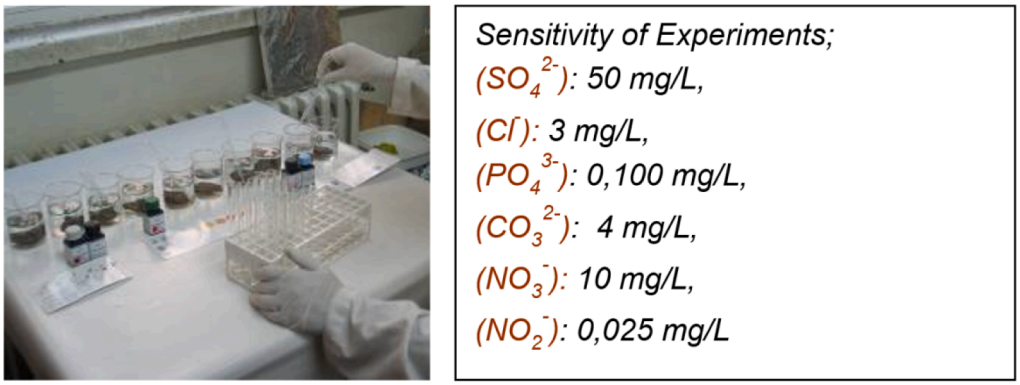

Fig. 12. **(a)** Spot salt experiments in the laboratory **(b)** Sensitivity of experiments list.

3.1.2. Investigation of acidic Aggregate, binder Analysis, and aggregate Granulometry

To identify the aggregate and binder parts of the mortar and plaster samples, the samples were first weighed dry before treatment with dilute acid (5 % HCl) to remove their binder (all carbonate content; CO_3^{2-}) contents (Fig. 13-a).

$$CO_3^{2-}{}_{(aq)} + 2HCl_{(aq)} \rightarrow CO_{2\,(g)} + Cl^-{}_{(aq)} + H_2O_{(s)}$$

The mortar and plaster samples were separated from the lime to obtain all the carbonate contents (binder) and aggregate part by filtration (Fig. 13-b), washing, and drying (Fig. 13-c). These were weighed again after drying at room temperature to calculate the total binder and aggregate by weight (% w/w) (Table 4 and Fig. 22). The aggregates of the samples (except those containing carbonate) were also systematically sifted to determine the aggregate particle distributions (granulometric analysis) (Table 4 and Fig. 22). This procedure was applied to all plaster and mortar samples (original or repaired) that responded to this type of analysis [52].

3.2. Polarized optical microscope analysis

Thin sections of the two case structures were prepared specifically the stone/rock, mortar, plaster, and ceramic (tiles and bricks) samples for examination under an optical microscope. Thin sections of the samples prepared for petrographic micromorphological studies, and also to show all layers from the material's surface to the interior. These examinations were conducted with a LEICA Research Polarizing Microscope Model DMLP top and bottom-illuminated optical microscope connected to a DFC280 digital camera (in parallel and crossed nicol with 2.5x magnification) (Fig. 14) [53].

3.3. FTIR Spectroscopy analysis

Due to the complexity of FTIR spectral data collecting, basic differences within samples may go unnoticed, hence feature extraction is essential (Fig. 15). The findings are more interpretable after using multivariate statistical analysis to minimize the number of variables acquired from the IR spectral data. In this study, a combination of verified and unverified approaches were used [38,39].

The aim of the material investigations of the structures using both individual laboratory and field analytical methodologies was to identify the effects of common weather events, such as snow, rain, and temperature change, and air pollution. One procedure detected the presence of water-soluble salts such as nitrate, nitrite, sulphate, phosphate, carbonate, and chloride, as well as their pH levels. This stage was crucial given the range of materials present, such as stone, earth, pottery, and mortar [40].

3.4. Resistivity measurement (RM)

To guarantee good contact, resistivity was tested using a Wenner series, comprising electrodes installed in small, drilled holes in empty spaces in the historic structure's garden. Resistivity (potential difference) was measured by passing an AC current through the two external electrodes and monitoring the tension between the two interior electrodes, performed multiple times at various places to increase reliability [30,31].

In this study, the data gathered using the Multi-Electrode ERT system (Fig. 16) was processed using Res2D-INV data processing software in the following ways: colour opacity scan, suitable resistivity scale, bad date control, Jacobien matrix control, and least square inverse solution method (3–10 times).

Imaging resistivity colour scale and mean resistivity (MR) values electrical resistivity testing can be used to detect the heritage area information, as shown in Fig. 17.

3.5. GPR survey

GPR is a well-known, commonly used NDT for evaluating structural condition. A transmitting antenna directs electromagnetic waves into the building, which are reflected back to a receiving antenna. The information recorded in the pulses is then examined to reveal hidden characteristics, such as cracks, material layers, delamination, leakage, and settlement. GPR is invaluable for revealing structural details, such as the subsurface geometry of the superstructure and the precise placement of the structural connections [33,54].

The main purpose of the present study was to find hidden cracks or moisture infiltration. A TR HF type 2 GHz GPR system was used for the survey (Fig. 18.a). To prepare for the GPR survey, conventional longitudinal and transverse surveys were painted on the surface with a temporary shadow, ensuring that the whole region was covered and that the data could be linked to specific locations (Fig. 18.b) [55].

The portable and manoeuvrable GPR instrument used for this work can record high-quality, densely surveyed data to produce high-grade tomography and 3D information. D tomography of the subsurface layers and 3D images of the measured capacity were created using IDS GRED data inspection software. A single tomographic map of the building was created by combining the longitudinal and transverse data.

3.6. Thermal imaging procedure

Thermal imaging involves using a thermal imaging camera to measure the absorption and emission of infrared light by the substance under investigation. Infrared radiation reveals that changes in sources were caused by heating and cooling processes triggered by variation in the ambient air temperature. The wavelength of the emitted radiation ranges from 0.75 to 10 μm, and is divided into spectrum bands that include visible light as well as microwaves [20,24]. The size of the sample determines the amount of radiation emitted. These emissions are captured by a thermal camera and shown as a coloured image. This method can demonstrate that a patch of defects between deep cracks is more vulnerable to temperature fluctuations because of its lower mass and larger surface area. A thermal imaging camera can use these response variations to detect the location of specific features. This type

Fig. 13. **(a)** Dilute acid purified samples **(b)** Filtered samples **(c)** Samples that were washed and dried.

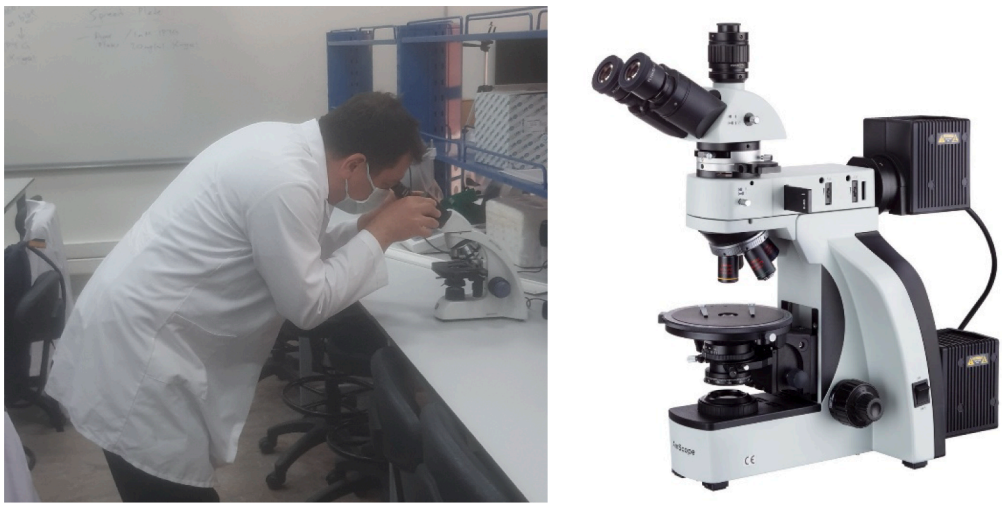

(a) (b)

Fig. 14. **(a)** Polarized optical Microscope in use, **(b)** Polarized optical microscope.

(a) (b)

Fig. 15. **(a)** FTIR Spectrometer in use, **(b)** FTIR spectrometer.

of examination can detect temperature changes as small as 0.08 °C, and is ideal for assessing temperature extremes. However, it should be noted that the findings can be skewed by wind, intense sunlight, and rain [56].

3.7. Finite element modelling

The purpose of numerical modelling is to determine the actual behaviour of a part or the whole of a structure, or structural system elements under different loads or conservational effects. The bearing system of historical buildings and monuments is often very complex, requiring many simplifications in order to model the building. To ensure a simple model, it is important to accurately define the mechanical properties of the materials that make up the carrier system elements [9].

The basic principles of an accurate finite element modelling are as follows:

- The simplest FE model always produces the greatest accuracy. Avoid using FE models that are more intricate and comprehensive than is necessary for the intended use and scope of the calculations.
- All structural effects required for the calculation should be considered when choosing the size and shape of the elements in the numerical model. For instance, in the structural analysis of an arch, the element representing the arch in the model should be chosen to allow computation of the axial force, shear force, bending moment, and torsion moment and the section characteristics should be established such that the results of these values are given. The model created by dividing a section of a larger model encompassing the complete structure is insufficient to evaluate the behaviour of an element or part in detail. For more detailed behaviour, models should accurately depict boundary conditions and connection patterns.

The numerical model, also called the Finite Element Model, is obtained by combining finite elements to reflect the behaviour of the entire structure. In finite element analysis, the most important factor is the individual behaviour of the elements that make up the model, followed by the behaviour of the entire numerical model [10].

Numerical modelling or mathematical modelling refers to the process of defining the structure, taking into account the geometric dimensions of the structure, the movement capabilities and degrees of freedom of the joints of the supports and structural system elements, and the loads acting on the structure. Fig. 19 shows the numerical models

Fig. 16. Ambergeo brand's Mangusta TMG 255 E model multi-electrode (48 electrode capacity) resistivity tomography device.

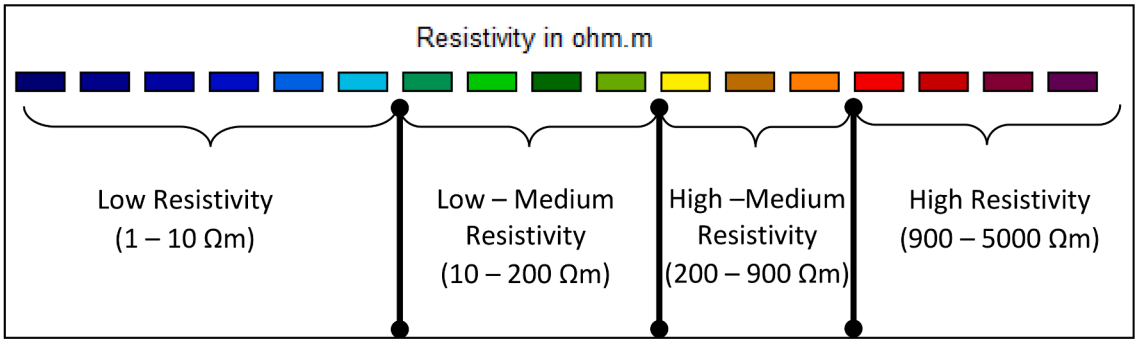

Fig. 17. Resistivity colour scale and mean resistivity (Ωm) values used in imaging.

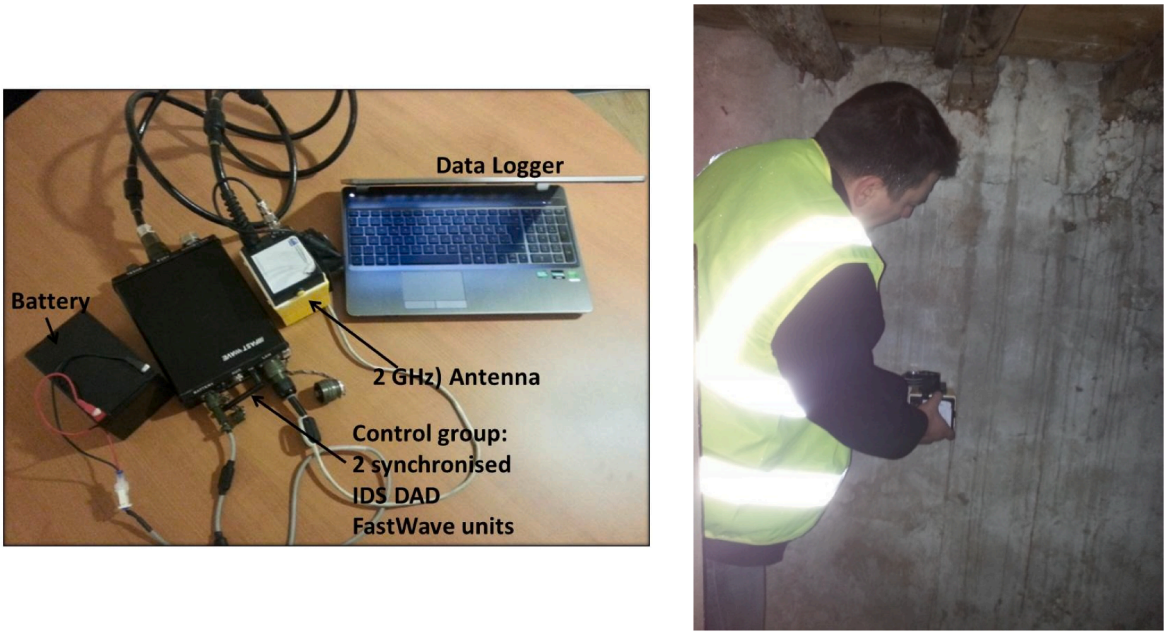

Fig. 18. **(a)** TR HF GPR antenna, **(b)** GPR in use.

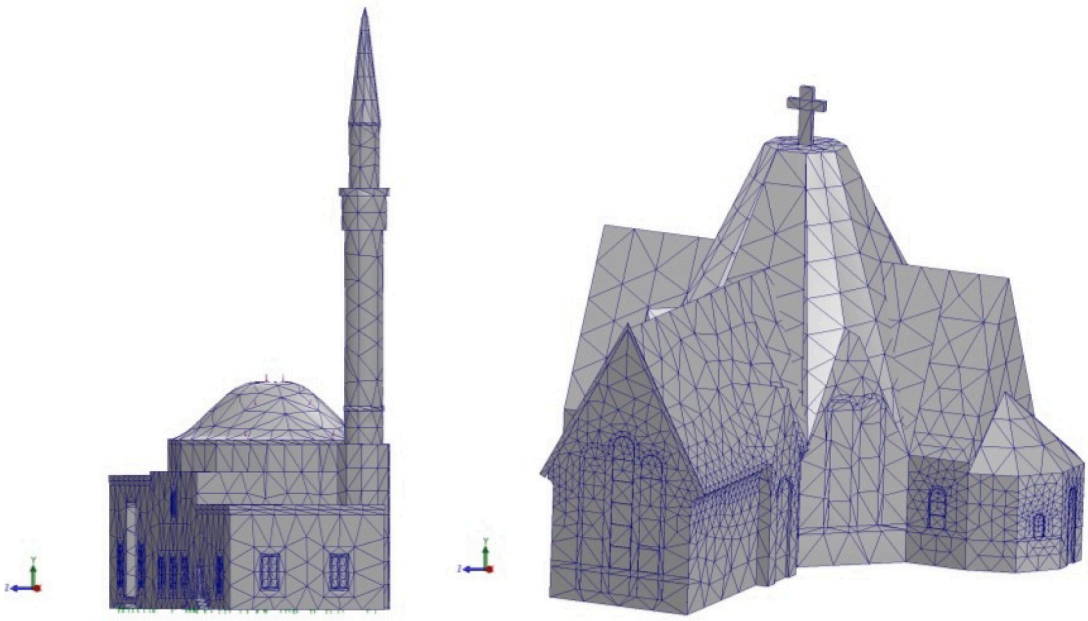

Fig. 19. Mesh of the Case Studies ANSYS model [14].

prepared to examine the earthquake resistance of the Case study Mosque and Church, respectively.

The behaviour of a relatively small portion of the material, often known as the differential element, determines assumptions about the mechanical characteristics of the construction material.. This differential element is used to produce the material model, which considers the stress–strain characteristics of the construction material. To construct an appropriate numerical model, it is crucial to thoroughly research the behaviour of both the material, and the individual components.

FEM modelling of structures is very challenging in structural analysis programs, and due to the church's detailed and complex structure, rather than modelling the whole structure, it was decided to model the main entrance and side combined structures separately. Linear and nonlinear analyses of the three-dimensionally modelled structure under static and dynamic loads are shown in the section 4.7. In the Fig. 20 below, some analyses for the main entrance and side combined structures are shown as examples.

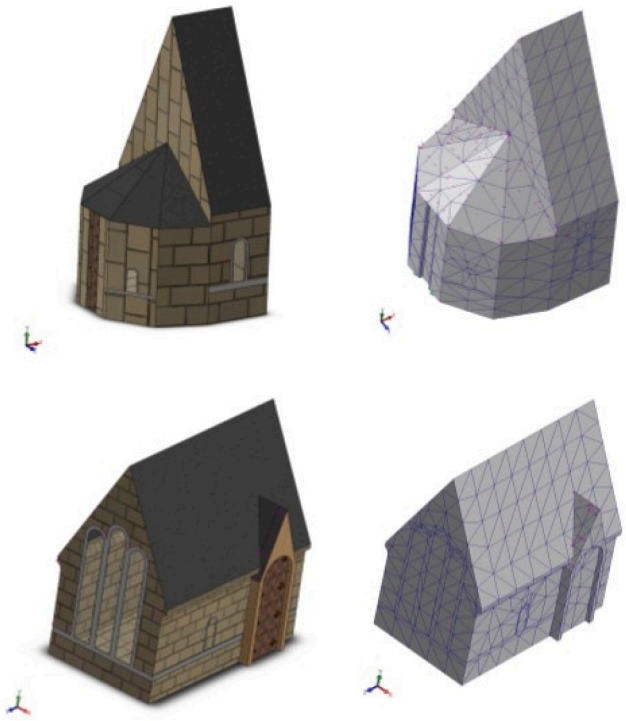

Fig. 20. Mesh of the split view Church ANSYS model [14].

4. Results

4.1. Laboratory material analysis results

4.1.1. Spot salt type Experiment results

All the examined stone samples of the two case study structures were acidic (pH $<$ 7), with pH values between 6.51 and 6.96 while the ceramic samples had a pH of 6.39. Stone samples produced more homogeneous pH values than ceramic samples. The brick sample from the case study 1 was notably acidic (Smp-M 4). Salt content analysis showed that stone and ceramic samples had high salt levels while the ceramic samples with high chlorine content also contained dissolved carbonate. Sulphation results in the stone and ceramic samples depended on the location, with higher sulphation in samples showing the salt effect of cement-containing repair plaster.

The water-soluble salt contents and types and the ambient pH values of the stone and ceramic (tile and bricks) specimens are given in Table 2. The amount of water-soluble salt (total) contained in the structure (pores) of the stone and ceramic (tile and bricks) materials in the structures studied was determined quantitatively (Table 3 and Fig. 21).

To determine the total salt levels, the samples were kept in 100 ml distilled water for 24 h before recording the salt content using a mode Neukum Serie 3001 conductometer.

4.1.2. Acidic Aggregate, binder Analysis, and aggregate Granulometry results

The aggregate and binder contents of the mortar and plaster samples could not be determined solely by acidic analysis, because, in addition to the lime, the carbonate-containing materials in the structures were purified with a binding function in mortars and plasters. Therefore, all carbonate-containing material purified by the acidic method was considered as a binder.

Table 2
Spot Salt Type Experiment Results.

Specimens	Nitrite (NO_2^-)	Nitrate (NO_3^-)	Phosphate (PO_4^{3-})	Carbonate (CO_3^{2-})	Sulfate (SO_4^{2-})	Chlorine (Cl^-)	pH
Smp-M 1	**0,050**	**10**	**0**	NONE	**200**	**3**	**6,69**
Smp-M 2	**0,075**	**25**	**0,200**	LITTLE	**200**	**60**	**6,57**
Smp-M 3	**0,025**	**10**	**0,100**	LITTLE	**400**	**18**	**6,78**
Smp-M 4	**0,025**	**10**	**0**	NONE	**400**	**6**	**6,86**
Smp-M 5	**0,025**	**10**	**0**	NONE	**400**	**6**	**6,86**
Smp-C 1	**0,050**	**10**	**0**	NONE	**400**	**3**	**6,65**
Smp- C 2	**0,050**	**10**	**0**	NONE	**200**	**3**	**6,51**
Smp- C 3	**0,025**	**75**	**0**	LITTLE	**200**	**250**	**6,39**
Smp- C 4	**0,025**	**10**	**0**	LITTLE	**400**	**60**	**6,92**
Smp- C 5	**0,025**	**75**	**0**	LITTLE	**200**	**100**	**6,96**

Table 3
Total Salt Dissolved in Water (SS%).

Samples	Total Salt (%)
Smp- M 1	1,52
Smp- M 2	0,68
Smp- M 3	1,07
Smp- M 4	1,52
Smp- M 5	1,53
Smp- C 1	1,84
Smp- C 2	1,12
Smp- C 3	1,79
Smp- C 4	0,84
Smp- C 5	1,43

The total aggregate and binder ratios were determined using the acidic treatment (Table 4 and Fig. 22).

4.2. Polarized optical microscope analysis

All samples were examined for textural, mineral type, condition, distribution, and particle size by petrographic thin/bright section optical microscope analysis. It was found that micro-fractures, cracks, and voids in the stone samples had been filled with recrystallized calcite. This substance had a structure that was low quality fired (800 °C) and low porosity (3 %), applied without sieving, homogeneously distributed, and with an angular fractured, ground, and coarse aggregate content (matrix total aggregate ratio = 30 %). The matrix contained quartz, calcite, limestone, and plagioclase, reflecting the local geology (Fig. 23).

4.3. FTIR Spectroscopy analysis

The rough surface layer of each ceramic fragment was scraped away

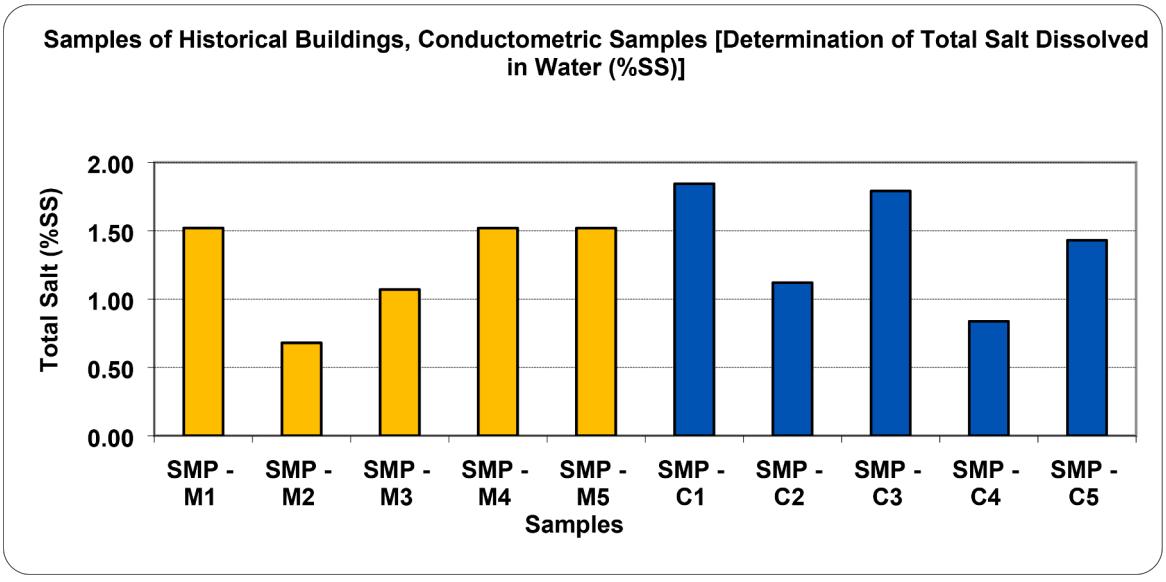

Fig. 21. Samples of Determination of Total Salt Dissolved in Water (%SS).

Table 4
Acidic Aggregate / Binder Analysis and Aggregate Granulometry.

Samples	Binding (%)	Agrega (%)	<63 µm	63–125 µm	125–250 µm	250–500 µm	500–1000 µm	greater than1000 µm
SMP –M 1	15,62	84,38	0,99	3,43	6,13	14,11	28,11	47,23
SMP –M 2	9,66	90,34	1,39	3,97	6,94	14,64	30,53	42,53
SMP –M 5	7,19	92,81	1,21	2,22	8,04	8,37	17,85	62,31
SMP –C 2	16,24	83,76	1,67	3,99	6,51	15,19	28,12	44,52
SMP –C 3	11,42	88,58	0,94	3	7,07	22,82	36,66	29,51
SMP –C 5	16,58	83,42	1,91	4,37	7,59	13,78	18,63	53,73

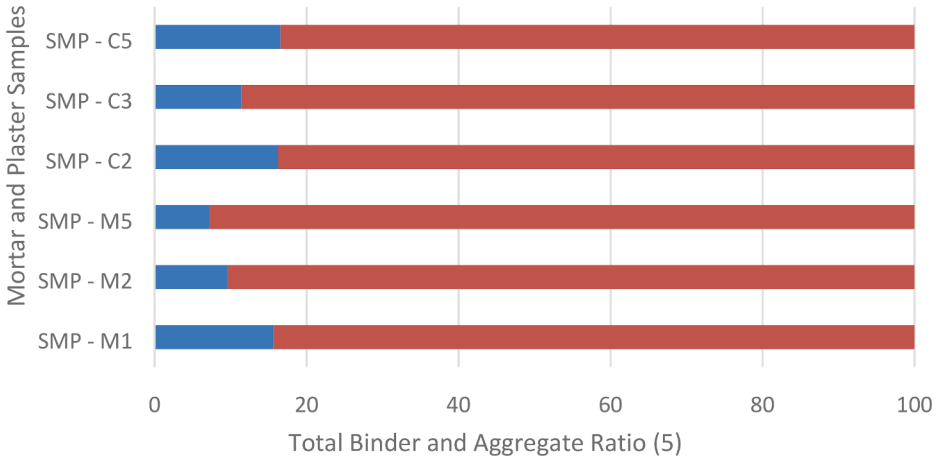

Fig. 22. Mortar and Plaster Samples of Acidic Aggregate / Binder Analysis.

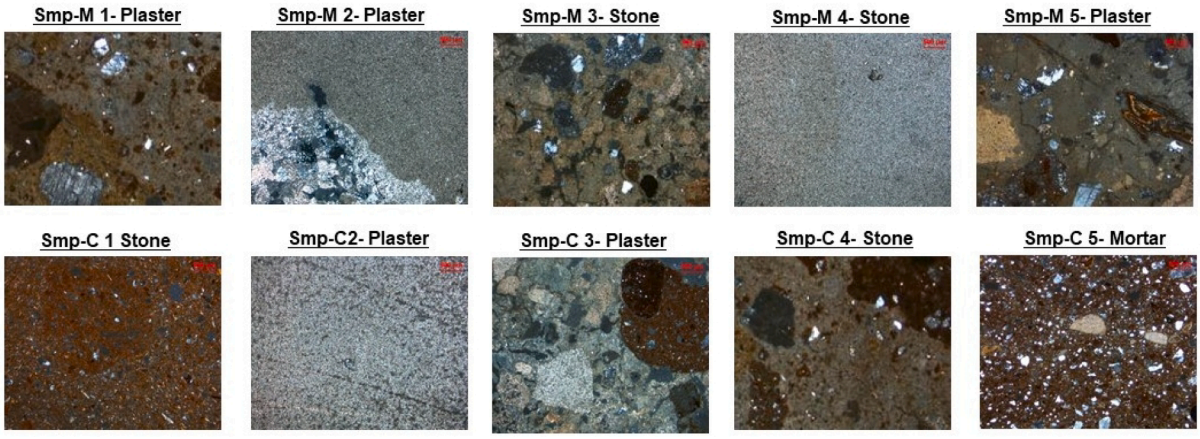

Fig. 23. Thin / Bright Section Polarized Optical Microscope Analysis.

to provide a smooth surface for FTIR spectroscopic examination. It was then washed with alcohol before a 1 mg sample was scraped. Based on the IR spectra, the samples had varying quantities of calcite (about 1150 cm^1) and quartz (596, 625, and 656 cm^1). Some samples included gypsum (ca. 2820, 3315, 1156, 1108, 640, and 618 cm^{-1}) or large amounts of calcite (ca. 2820, 3315, 1156, 1108, 640, and 618 cm^{-1}). Fig. 24 shows that the FTIR spectra for the interior and exterior surfaces of various samples varied. It shows the FTIR spectra of the sections with high calcite and gypsum levels, as well as revealing discrepancies between the exterior and the insides.

Previous investigations found that a range of old structures had comparable amounts of plant- and mineral-tempered stone in all samples [38]; in our investigation, in contrast, the top layers, contained far fewer mineral-tempered stone samples. The voids in the cross divisions, as seen in Fig. 24, suggest the use of organic temper. For mineral materials, coarse calcite grains may have been added to the clay raw material [39]. The analysis of the stone samples suggests that, these granules are either conventional, for example, carbonate sand, or purposely extracted from the stone samples, for example, by fracturing carbonate rocks or calcite veins.

4.4. Resistivity measurement (RM)

The data processing required the detailed evaluation of all data captured in the analysis. Based on the colours in the Colour Scale used in the RM result views acquired, and the resistivity values represented by these colours, it is possible to divide the colour scale as shown in Fig. 25.

4.5. GPR survey

The GPR scan of the two case study buildings provided the central cross-section of the radargram, displayed in Fig. 26. This clearly shows previous faults and material alterations. After a more individualized profile processing phase, spots in the data with strong reflectors were manually identified as areas of coarse fill materials inside the structure.

As Fig. 26 shows, the GPR receiving antenna recorded many radar rebounds, which risks have limiting and disguising the anomaly signals; nevertheless, the layers and sites where moisture infiltration caused damage are clearly distinguished. The case study 1showed differences in the façade's masonry with the inner and outer stone faces hiding a rubble core in the investigated section. The inconsistencies in the ashlar face described in the case study 2 was probably caused by cracks, voids, or poor mortar.

4.6. Thermal imaging

Thermal imaging inspection revealed concrete deterioration, cover delamination, water seepage, and significant fractures.

Thermal imaging also revealed the case study 1 and 2 mural's delamination and objectivities. The presence of stored heat (Fig. 27) suggested that splits had occurred within the cracks in this area, requiring immediate repair to avoid further deterioration or even irreversible damage.

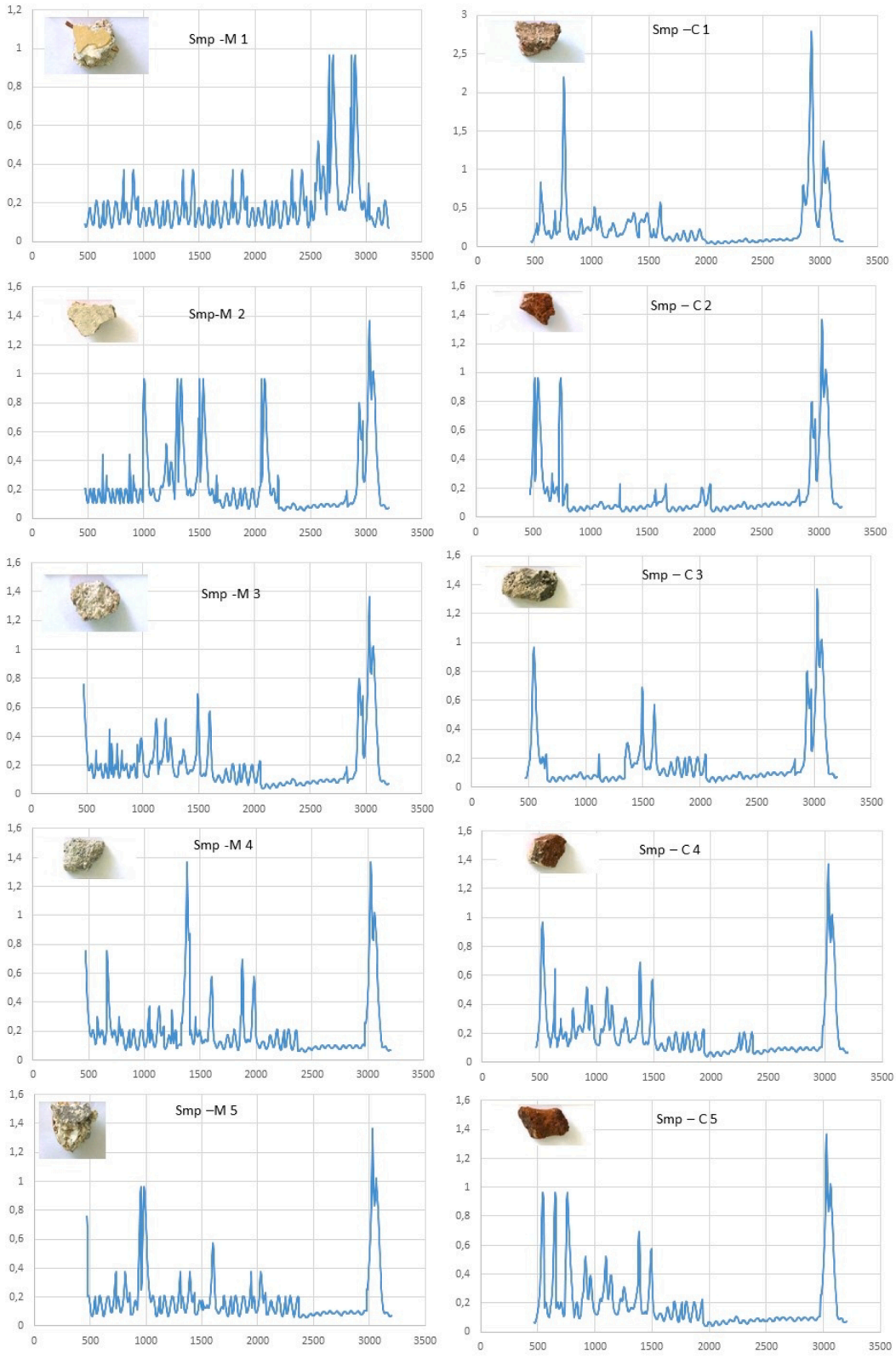

Fig. 24. FTIR Spectra of the samples.

4.7. FE modelling results

The proper evaluation and comprehension of the calculated findings will be aided by a well-organized presentation of the results. There are a great many degrees of freedom in a medium-sized finite element model of a historic structure, and it is difficult to simultaneously analyse all results in a single file. The deformations of the finite element model created for structural analysis under applied loads provide the clearest explanation of the calculation results and the behaviour of the structure. Fig. 28 depicts the altered state of the Church and Mosque case study, which was examined using the finite element approach.

Finite element computer programs display shear stresses,

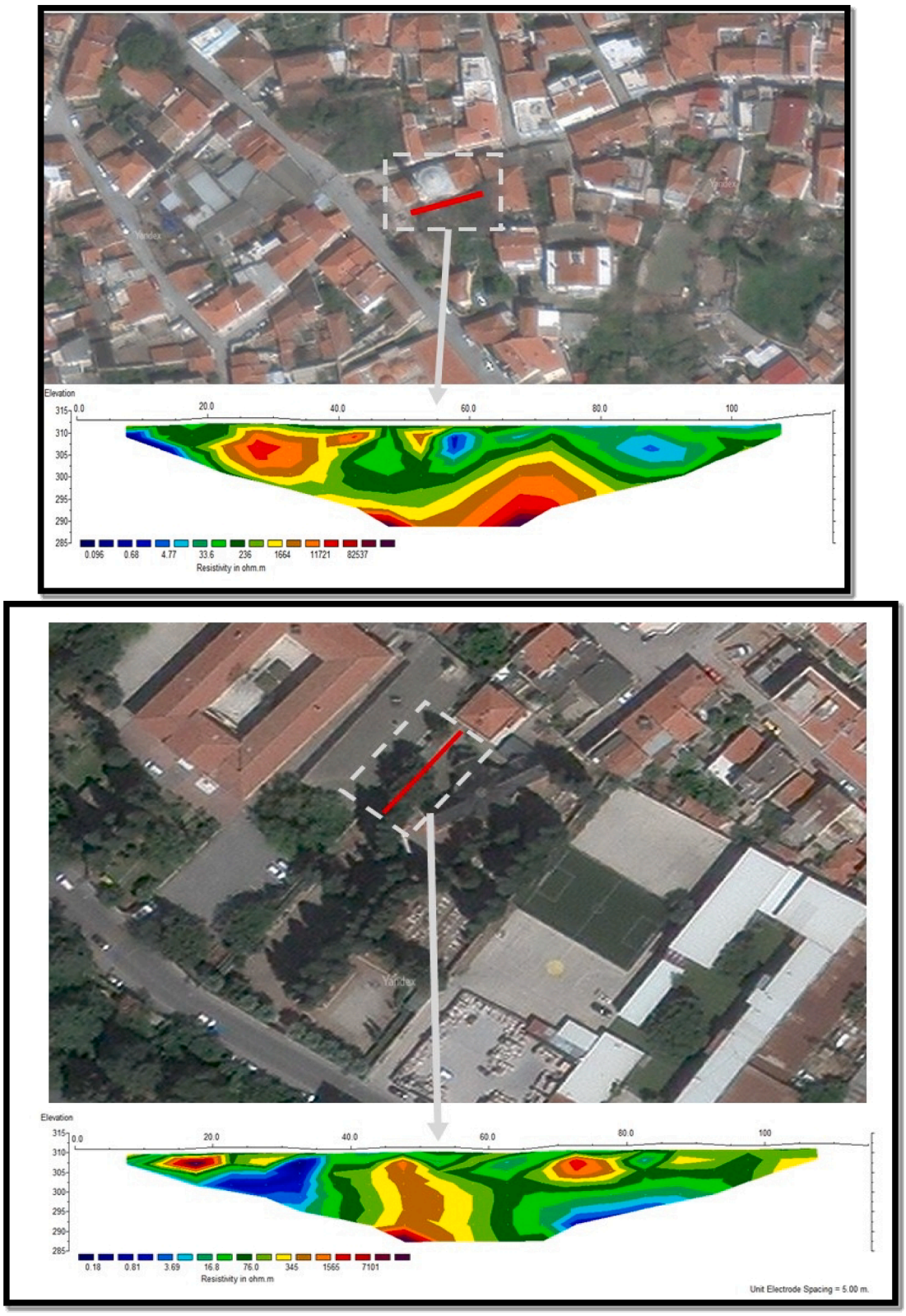

Fig. 25. Resistivity measurement (RM) results.

compressive and tensile stresses with colour contours, and this allows easy identification of the areas of the building posing a bearing capacity danger in the face of earthquake or other load effects. If necessary, more detailed calculations for these regions can be made with the previously mentioned micro modelling method.

5. Discussion

This study examined the status of two historic structures in western Turkey following an earthquake on Samos Island in Greece. In the absence of blueprints or other documentation, structural evaluations were needed to assess their current state. This was achieved by

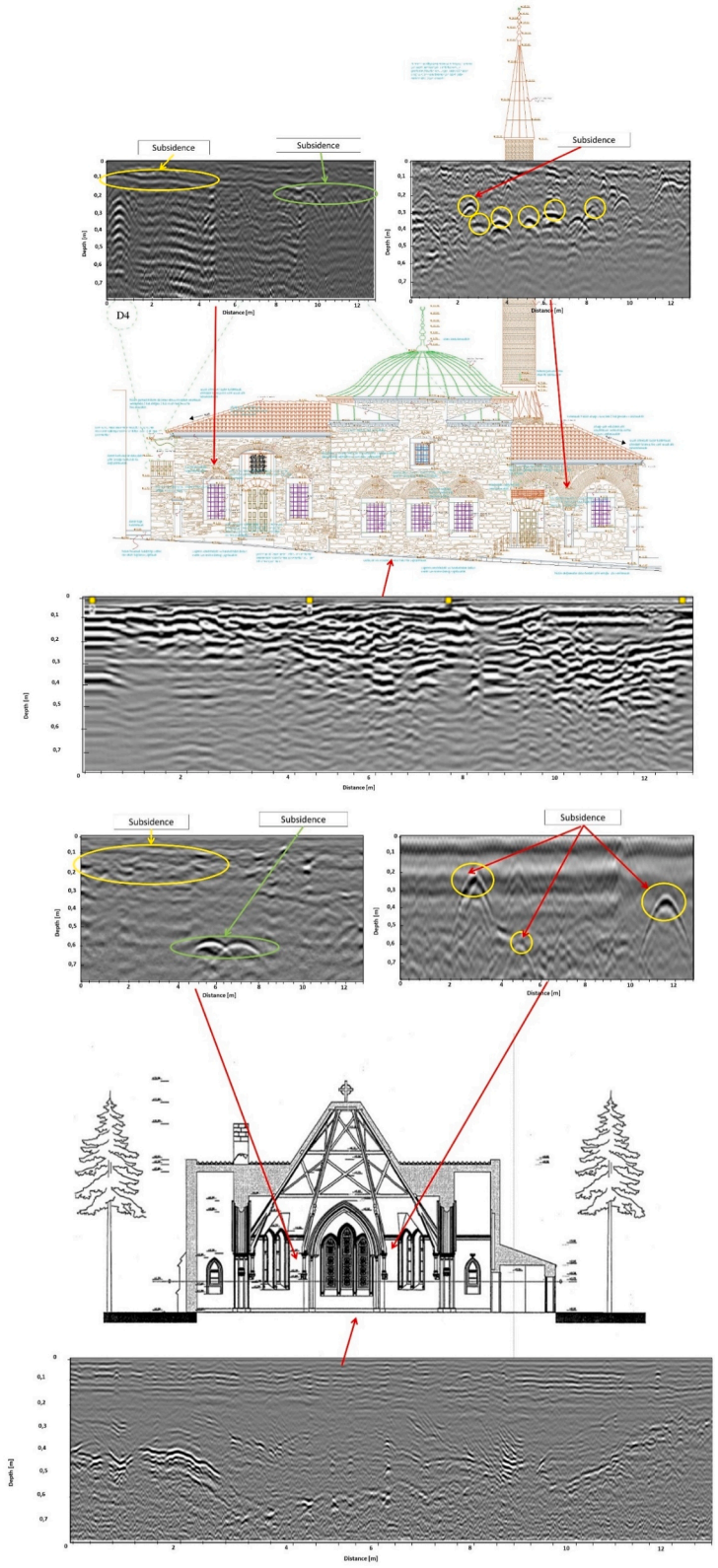

Fig. 26. Processed GPR Radargram Data and Possible Interpretations.

combining data from the following inspection methods: visual inspection, GPR, RM, and infrared thermography, laboratory analysis, polarized optical microscope analysis, and FTIR. These combined approaches created a comprehensive view of the current state of the two buildings, to inform judgments on necessary corrective work [40,54].

The findings highlight the need for a multi-disciplinary approach to such surveys, especially in the case of structures with little or no structural record. The variety of methodologies available undoubtedly increases the complexity of assessment; however, the strategy used in this study shows that this complexity can become manageable using a combination of NDT and other analyses eliminating the need for further tests [25,27,36].

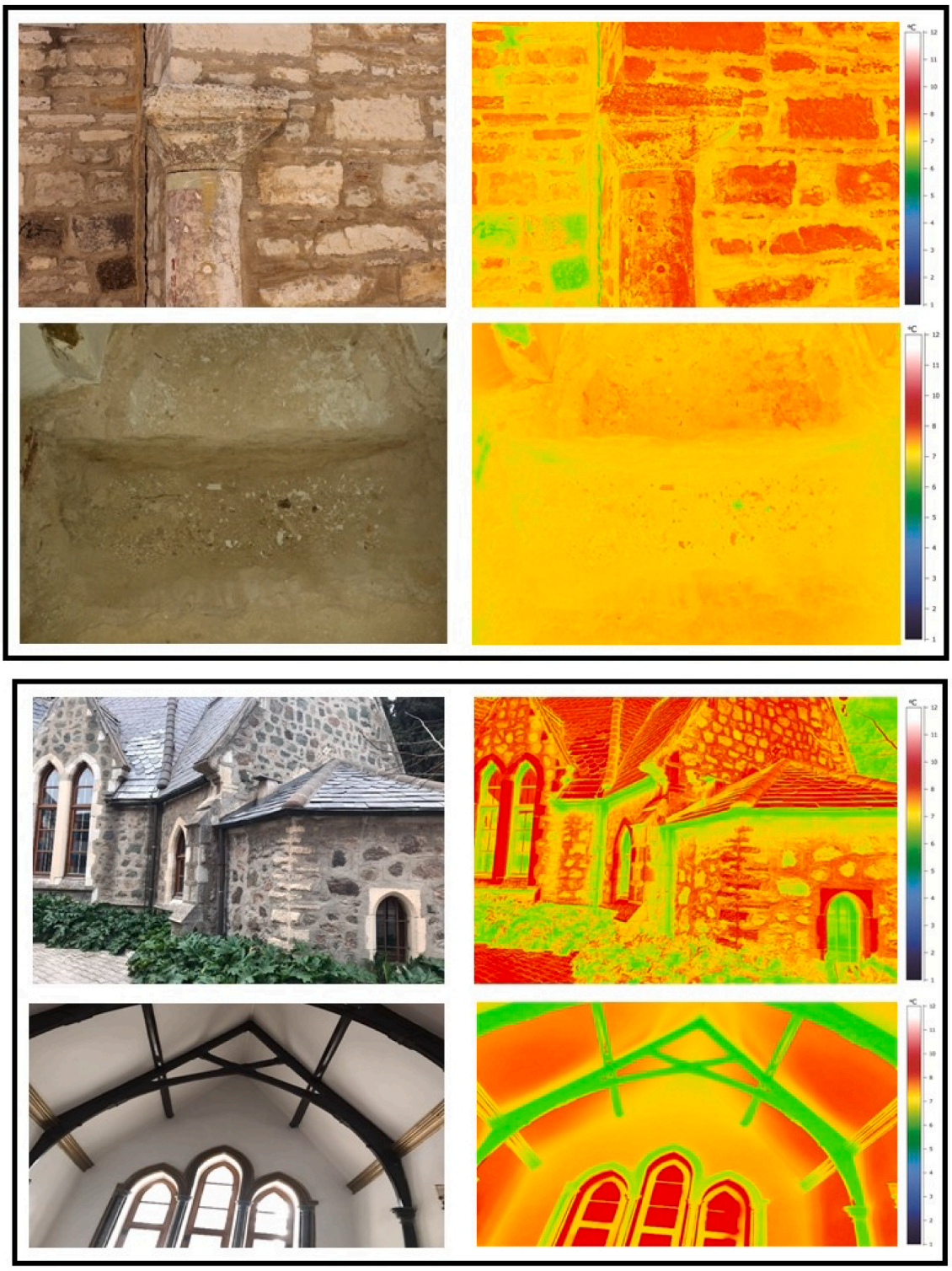

Fig. 27. Thermal imaging results.

In this study, laboratory analysis was used to determine the water-soluble salt types (nitrate, nitrite, sulfate, phosphate, carbonate, and chlorine) and the pH values of the stone and ceramic (tile and brick) specimens sampled from the two case study structures. The samples were all acidic (pH 7) in nature. The conductometric analysis revealed greater salt content in the ceramic samples than the rock/stone samples. The aggregate structure in the lower-layer plaster samples was more homogenous than in the upper-layer samples, demonstrating changes in the contents of the upper-layer plaster over time. All samples were analysed for texture, mineral type, condition, distribution, and particle size using a petrographic brilliant thin-section optical microscopy. Petrographic analysis was used to identify stone and ceramic materials within the structures, as well as the aggregate and binder composition of the mortars and plasters, and their structural qualities [48].

The petrographic analysis of the formation sources of the rock and stone samples revealed very uniform micritic limestone, typical of the

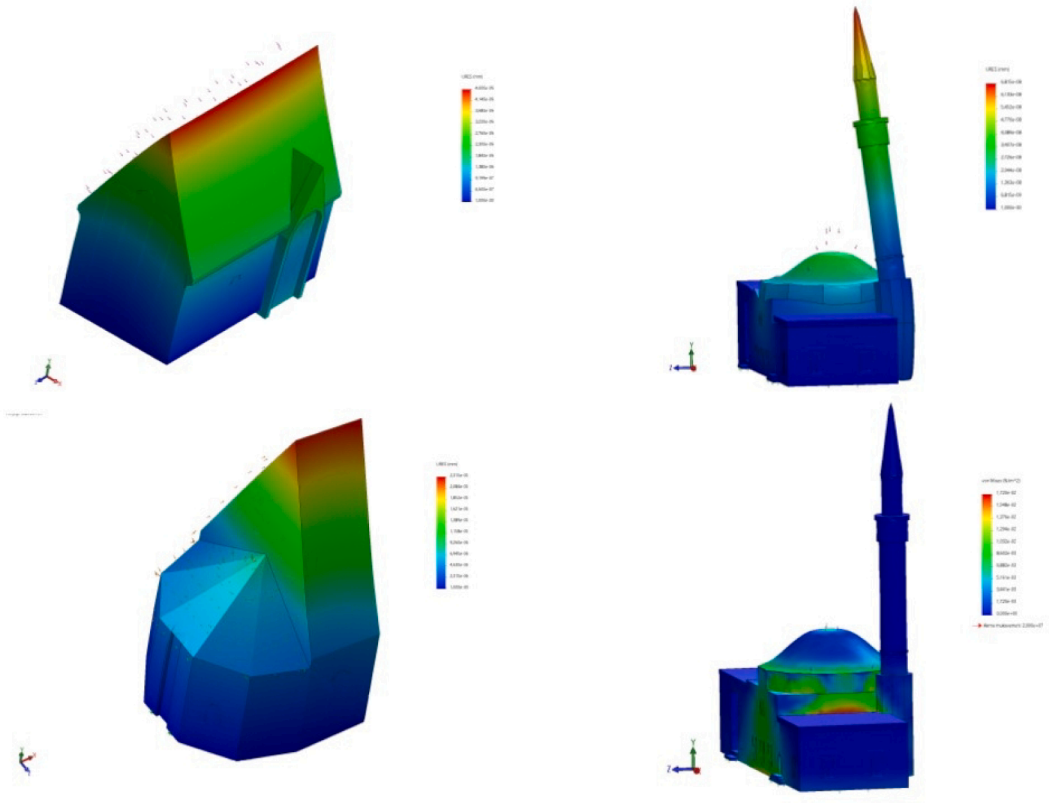

Fig. 28. Maximum stresses developed at the walls of Church and Mosque in coloured contours.

local formation in Izmir and its surroundings. The limestone used in the construction therefore certainly originated from Izmir region. Thus, for stone repairs, rock of the same type, texture, and petrographic properties should be obtained from sources local to Izmir. For restoration, it is recommended that locally-sourced equivalent rock samples (travertine) should be obtained, and subjected to petrographic analysis to ensure that their properties match those in the original structure (Fig. 29) [57].

6. Conclusions

Following the Samos Island earthquake in 2020, this study examines the role of innovative NDT in the identification of the structural condition of two historic buildings in western Turkey. The results contribute significantly to our understanding of the conservation of cultural heritage, thereby supporting its long-term preservation.

This earthquake's high dynamic load provided an opportunity to evaluate the seismic performance of various structures in Izmir province. The key feature of the earthquake was the strength of ground

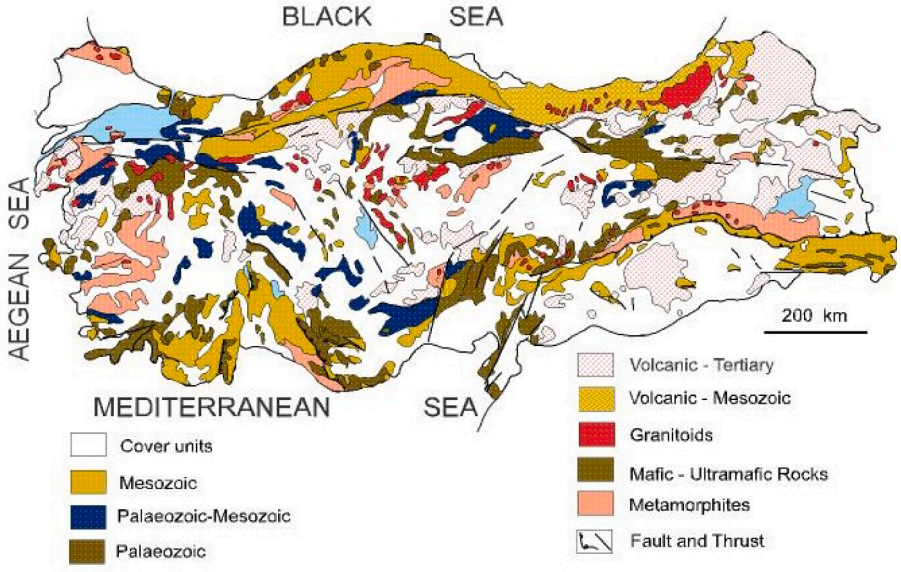

Fig. 29. Formation sources of rock and stone in Turkey [57].

vibrations which affected soft ground more than 70 km from the epicentre. The damage varied across comparable structures exposed to identical ground motion levels [1–4]. This study focused on the specific effects of this earthquake on two historic structures, using sophisticated NDT evaluations and laboratory studies. Fortunately, neither historic building collapsed or sustained substantial damage, unlike several other structures in the region. Given the present level of earthquake risk, these other damaged structures failed to meet the existing seismic safety requirements as stipulated in regulations. Thus, the earthquake's different effects highlights the dangers for weaker structures, and underlines the urgency of taking action to improve their condition to ensure their future safety.

Structural health assessment has become a major focus of structural engineering due to recent advances in NDT equipment, data processing, and structural identification. Although the technical development of this approach is still in its early phases, there are clear indications that structural health assessment will soon supplant traditional constant conservation strategies [20, 22, 27,]. Currently, following an earthquake, a standardized structural health assessment is generally preferred due to its low intrusiveness and widely-accepted destruction assessment capabilities. Nonetheless, it is well recognized that such approaches are unable to fully identify local defects, which, regardless of size, may nevertheless affect structural rigidity. Recent studies have therefore recommended the adoption of integrated monitoring systems, in which data from multiple NDTs are analysed simultaneously to produce a complete structural evaluation. Despite significant advances in these systems, practitioners continue to face considerable challenges in practical application. This study describes the application of various NDT solutions and laboratory analyses that can reduce these challenges, as well as proposing methodological and scientific improvements for long-term structural health monitoring.

The first inspection discovered significant cracking and other problems while further investigation using GPR and RM revealed more detailed information concerning cracks, wetness, and identifiable soil layers in various locations. By combining GPR, RM, and intrusive testing, it was possible to identify the areas of greatest risk of water infiltration. Finally, infrared thermography from a distance allowed the detection of deterioration locations, such as significant sub-surface cracking and detachment pieces in the mural areas. This combination of methods ensured quick feedback, allowing real-time decision-making.

Both buildings have an unsymmetrical, elongated construction style. In the analysis of the mosque structure under its own weight, it has been determined that the maximum vertical displacement occurs in the dome's central section. For the church structure, in the earthquake analyses in the y and z directions, high stress values were found only at the arch end regions. In the stress analyses, stress levels approach the boundary stress values in the regions where the load is transferred to the walls in the sections of both the mosque and the church. It has been determined that, in these regions, additional stresses will cause excessive boundary stress values, creating risk. This integrated strategy makes it, possible to find ways to greatly reduce the impact of masonry degradation and aging on the mosque and church structure's ability to support its own weight.

Experimental, in-situ, and laboratory studies have shown significant variation in the physical and mechanical characteristics of ancient masonry, for example, inside a masonry wall or a masonry pier, and therefore, it is difficult to determine the load-bearing capacity of these historic masonry structures. This is because of the heterogeneity of masonry, the variability of the properties of its various components, irregularities in its execution, moisture distribution, or level of degradation, as well as the dispersion of values obtained by diagnostic methods of the detection of compressive strength of masonry units and mortars. The issue of ultimate or acceptable load-bearing capability become important in cases of severe masonry degradation, rebuilding entailing a change in loading, or significant interventions made to existing masonry. For structural engineers and academics, this research contributes to the body of knowledge on our understanding of ancient structures' behaviour in terms of their functionality, stability, and durability (Fig. 30).

The FEM results of laboratory analysis can be combined polarized optical microscope analysis, FTIR spectral data analysis, and advanced techniques such as GPR, thermal imaging, and RM. These combined results imply that that primary steps in maintaining the condition of built masonry are proper maintenance, preventive measures, and monitoring. This combined method could lead to the substantial reduction of the impact of masonry damage and aging on the structure's ability to support loads [58,59]. Following a thorough analysis of the Church and Mosque case studies, the following primary findings about mechanical characteristics can be drawn:

- The decay and aging of brickwork masonry significantly impact the mechanical qualities of both church and mosque masonry elements, as well as masonry as a composite material. Moisturizing, capillary rise, and freezing-thawing cycling were likely the most potent factors accelerating masonry degradation in both case studies.
- Prior to using more invasive procedures to assess mechanical qualities, a thorough inspection of the built-in masonry components is required. It is important to consider the amount of water that can be absorbed by a specific type of brick used in the masonry when evaluating the structure's moisture content.
- The intruding water causes the mobilization and production of salts due to capillary rise and moistening. Salts are potent destructors that can damage porous building materials by processes such as osmosis, hydration, differential thermal expansion, and crystallization. Any of these processes can greatly influence characteristics of the mortar and masonry bond. In damp conditions, the masonry's modulus of elasticity is quite low, comparable to that of saturated sand.

The structural components of the two historic structures were damaged to varying degrees, as indicated by the building materials (laboratory and NDT tests). Also, recent repairs to the structures used inappropriate materials (mortars and plasters containing cement). Based on the identification of original mortar and plaster samples, the following recommendations can be made for the repair process:

- Lime mortar should be used for joint repairs and crack filling in the building's façade masonry. This should contain 25 percent lime by weight, 45 percent toothed/fractured, sieved, washed, with an aggregate distribution consistent with the original mortar (39 percent max. 1–2 mm coarse, 60 percent 63–1000 m grained silt/sand, and 1 percent). The recommendation is for lime mortar with a silt/clay combination with 63 m grains at a rate of 63 m) and rock-free aggregate with carbonate content, crushed and sieved limestone fragments at 20 percent, and brick fragments at 10 percent. In terms of strength, the use of broken bricks is completely adequate in internal plasters and in external mortars, but organic additions in the original mortar are not advised.
- It is not recommended to use of cement-containing materials (classical, white, or all types of pigment-coloured cement) at any stage in the repair of mortar and plaster components. Trial applications should be conducted and monitored to check whether the newly-introduced mortar and plaster contents are compatible with the original material.

To the best of the author's knowledge, this is the first study of its kind. Hence, it makes a substantial contribution to the field, specifically by showing how a structural evaluation method integrating a limited selection of tests can provide consistent information on both visible and hidden faults affecting the integrity of historic structures. This technique provides highly reliable information regarding concealed features, allowing appropriate maintenance programs to be developed in the absence of original construction documents. The multidisciplinary

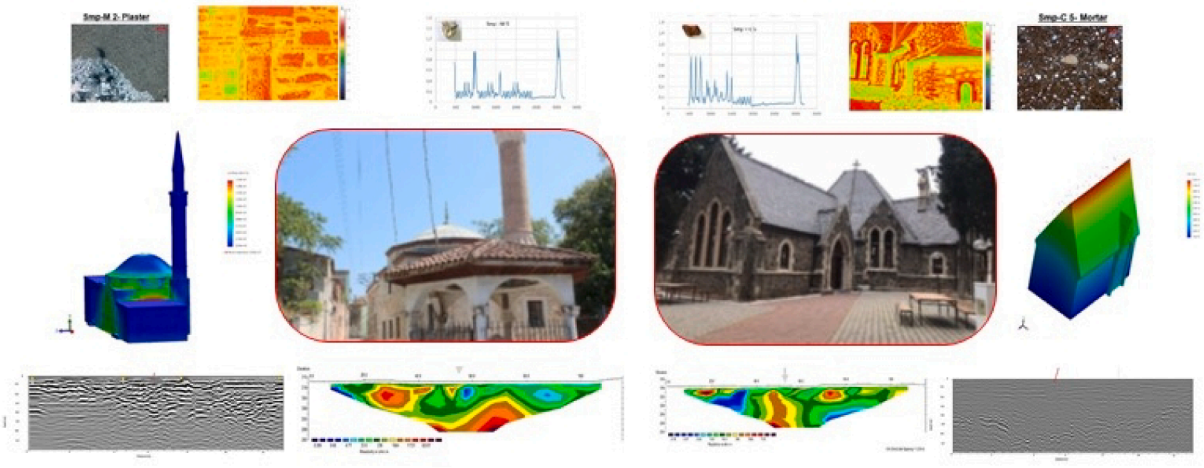

Fig. 30. Integrated approach on the Church and Mosque case studies.

approach implemented enables an extensive evaluation of the structural health and future needs of historic structures, with great potential for use in similar circumstances. Thus, the study makes a significant contribution to the body of knowledge, particularly to specialists' operational information regarding historic building stability and durability.

The structural components of the two historic structures were damaged to varying degrees, as indicated by the building materials (laboratory and NDT tests). Also, recent repairs to the structures used inappropriate materials (mortars and plasters containing cement). However, identification of original mortar and plaster samples can guide the repair process, leading to following recommendations:

- Lime mortar should be used for joint repairs and crack filling of the building's façade masonry. This should contain 25 percent lime by weight, 45 percent toothed/fractured, sieved, washed, with an aggregate distribution consistent with the original mortar (39 percent max. 1–2 mm coarse, 60 percent 63–1000 m grained silt/sand, and 1 percent). The recommendation is for lime mortar with a silt/clay combination with 63 m grains at a rate of 63 m) and rock-free aggregate with carbonate content, crushed and sieved limestone fragments at 20 percent, and brick fragments at 10 percent. In terms of strength, the use of broken bricks is completely adequate in internal plasters in external mortars, but organic additions in the original mortar are not advised.
- The use of cement-containing materials (classical, white, or all types of pigment-coloured cement) is not recommended for any stage in repairing mortar and plaster components. Trial applications should be conducted and monitored to check whether the newly-introduced mortar and plaster contents are compatible with the original material.

To the best of the author's knowledge, this is the first such of its kind. Hence, it makes a substantial contribution to the field, specifically by showing how a structural evaluation method integrating a limited selection of tests can provide consistent information on both visible and hidden faults affecting the integrity of historic structures. This technique provides highly reliable information regarding concealed features, allowing appropriate maintenance programs to be developed in the absence of original construction documents. The multidisciplinary approach implemented enables an extensive evaluation of the structural health and future needs of historic structures, with great potential for use in similar circumstances. Thus, the study makes a significant contribution to the body of knowledge, particularly to specialists' operational information regarding historic building stability and durability.

Declaration of Competing Interest

The authors declare that they have no known competing financial interests or personal relationships that could have appeared to influence the work reported in this paper.

References

[1] Gülerce Z, Akbaş B, Özacar AA, Sopacı E, Önder FM, Uzel B, et al. Samos Earthquake, Soil Dynamics and Earthquake Engineering, Volume 152, 2022. ISSN 2020;107053:0267–7261. https://doi.org/10.1016/j.soildyn.2021.107053.

[2] Cetin K.O., Altun S., Askan A., Akgün M., Sezer A., Kıncal C., Özdağ Ö. C., İpek Y., Unutmaz B., Gülerce Z., Özacar A. A., Ilgaç M., Can G., Cakir E., Söylemez B., El-Sayeed A., Zarzour M., Bozyiğit İ., Tuna Ç., Köksal D., Karimzadeh S., Uzel B., Karaali E., The site effects in Izmir Bay of October 30 2020, M7.0 Samos Earthquake, Soil Dynamics and Earthquake Engineering, Volume 152, 2022, 107051, ISSN 0267-7261, https://doi.org/10.1016/j.soildyn.2021.107051.

[3] Mavroulis S, Ilgac M, Tunçağ M, Lekkas E, Püskülcü S, Kourou A, et al. Emergency response, intervention, and societal recovery in Greece and Turkey after the 30th October 2020, MW = 7.0, Samos (Aegean Sea) earthquake. Bull Earthquake Eng 2022;20(14):7933–55.

[4] Tepe Ç, Sözbilir H, Eski S, Sümer Ö, Özkaymak Ç. Updated historical earthquake catalog of İzmir region (western Anatolia) and itsimportance for the determination of seismogenic source. Turk J Earth Sci 2021;30(SI-1):779–805.

[5] Valluzzi MR, Modena C, de Felice G. Current practice and open issues in strengthening historical buildings with composites. Mater Struct 2014;47:1971–85. https://doi.org/10.1617/s11527-014-0359-7.

[6] Kor E., Ozcelik Y., Seismic performance assessment of concentrically braced steel frames designed to the Turkish Building Earthquake Code 2018, Structures, Volume 40, 2022, Pages 759-770, ISSN 2352-0124, https://doi.org/10.1016/j.istruc.2022.04.033.

[7] Can G., Askan A., Karimzadeh S., An assessment of the 3 February 2002 Cay (Turkey) earthquake (Mw=6.6): Modeling of ground motions and felt intensity distribution, Soil Dynamics and Earthquake Engineering, Volume 150, 2021, 106832, ISSN 0267-7261, https://doi.org/10.1016/j.soildyn.2021.106832.

[8] Appiotti F, Assumma V, Bottero M, Campostrini P, Datola G, Lombardi P, et al. Definition of a Risk Assessment Model within a European Interoperable Database Platform (EID) for Cultural Heritage. J Cult Herit 2020;46:268–77.

[9] Ravankhah M., Schmidt M., Will T., An indicator-based risk assessment framework for World Heritage sites in seismic zones: The case of "Bam and its Cultural Landscape" in Iran, International Journal of Disaster Risk Reduction, Volume 63, 2021, 102405, ISSN 2212-4209, https://doi.org/10.1016/j.ijdrr.2021.102405.

[10] Pianigiani M, Careccia C, Montone C. Correlation analysis between churches and their artistic content in terms of damage. A damage map of Italian Cultural Heritage through four Regions after the 2016 earthquake. Procedia Struct Integrity 2020;29:103–10. https://doi.org/10.1016/j.prostr.2020.11.145. ISSN 2452–3216,.

[11] Maio R, Ferreira TM, Vicente R. A critical discussion on the earthquake risk mitigation of urban cultural heritage assets. Int J Disaster Risk Reduct 2018;27:239–47. https://doi.org/10.1016/j.ijdrr.2017.10.010. ISSN 2212–4209,.

[12] Biglari M., Formisano A., Davino A., Seismic vulnerability assessment and fragility analysis of Iranian historical mosques in Kermanshah city, Journal of Building

Engineering, Volume 45, 2022, 103673, ISSN 2352-7102, https://doi.org/10.1016/j.jobe.2021.103673.
[13] Işık N., Halifeoğlu F. M., İpek S., Detecting the ground-dependent structural damages in a historic mosque by employing GPR, Journal of Applied Geophysics, Volume 199, 2022, 104606, ISSN 0926-9851, https://doi.org/10.1016/j.jappgeo.2022.104606.
[14] Ashayeri I., Biglari M., Formisano A., D'Amato M., Ambient vibration testing and empirical relation for natural period of historical mosques. Case study of eight mosques in Kermanshah, Iran, Construction and Building Materials, Volume 289, 2021, 123191, ISSN 0950-0618, https://doi.org/10.1016/j.conbuildmat.2021.123191.
[15] Illampas R., Ioannou I., Lourenço P. B., Seismic appraisal of heritage ruins: The case study of the St. Mary of Carmel church in Cyprus, Engineering Structures, Volume 224, 2020, 111209, ISSN 0141-0296, https://doi.org/10.1016/j.engstruct.2020.111209.
[16] Proença JM, Gago AS, Vilas BA. Structural window frame for in-plane seismic strengthening of masonry wall buildings. International Journal of Architectural Heritage 2019;13(1):98–113. https://doi.org/10.1080/15583058.2018.1497234.
[17] Bal İE, Dais D, Smyrou E, Sarhosis V. Monitoring of a Historical Masonry Structure in Case of Induced Seismicity. International Journal of Architectural Heritage 2021;15(1):187–204. https://doi.org/10.1080/15583058.2020.1719230.
[18] Dais D., Bal İ.E., Smyrou E., Sarhosis V., Automatic crack classification and segmentation on masonry surfaces using convolutional neural networks and transfer learning, Automation in Construction, Volume 125, 2021, 103606, ISSN 0926-5805, https://doi.org/10.1016/j.autcon.2021.103606.
[19] Diz-Mellado E., Mascort-Albea E. J., Romero-Hernández R., Galán-Marín C., Rivera-Gómez C., Ruiz-Jaramillo J., Jaramillo-Morilla A., Non-destructive testing and Finite Element Method integrated procedure for heritage diagnosis: The Seville Cathedral case study, Journal of Building Engineering, Volume 37, 2021, 102134, ISSN 2352-7102, https://doi.org/10.1016/j.jobe.2020.102134.
[20] Fort R, Alvarez de Buergo M, Perez-Monserrat EM. Non-destructive testing for the assessment of granite decay in heritage structures compared to quarry stone. Int J Rock Mech Min Sci 2013;61:296–305.
[21] Tejedor B., Lucchi E., Bienvenido-Huertas D., Nardi I., Non-destructive techniques (NDT) for the diagnosis of heritage buildings: Traditional procedures and futures perspectives, Energy and Buildings, Volume 263, 2022, 112029, ISSN 0378-7788, https://doi.org/10.1016/j.enbuild.2022.112029.
[22] Yalçıner C. Ç., Büyüksaraç A., Kurban Y. C., Non-destructive damage analysis in Kariye (Chora) Museum as a cultural heritage building, Journal of Applied Geophysics, Volume 171, 2019, 103874, ISSN 0926-9851, https://doi.org/10.1016/j.jappgeo.2019.103874.
[23] Navacerrada M.A., Barbero-Barrera M.M., Fort R., Prida D. de la, Núñez J.C., Gómez T.S., Application of acoustic impedance gun to non-destructively monitor stone damage, Construction and Building Materials, Volume 323, 2022, 126510, ISSN 0950-0618, https://doi.org/10.1016/j.conbuildmat.2022.126510.
[24] Moropoulou A, Labropoulos KC, Delegou ET, Karoglou M, Bakolas A. Non-destructive techniques as a tool for the protection of built cultural heritage. Constr Build Mater 2013;48:1222–39. https://doi.org/10.1016/j.conbuildmat.2013.03.044. ISSN 0950–0618,.
[25] Alexakis E, Delegou ET, Lampropoulos KC, Apostolopoulou M, Ntoutsi I, Moropoulou A. NDT as a monitoring tool of the works progress and the assessment of materials and rehabilitation interventions at the Holy Aedicule of the Holy Sepulchre. Constr Build Mater 2018;189:512–26. https://doi.org/10.1016/j.conbuildmat.2018.09.007. ISSN 0950–0618,.
[26] Wang L., Ren G., Hua F., Young S. S., Wang W., Yang C., Zhu J., Integrating habitat availability into restoration efforts for biodiversity conservation: Evaluating effectiveness and setting priorities, Biological Conservation, Volume 257, 2021, 109127, ISSN 0006-3207, https://doi.org/10.1016/j.biocon.2021.109127.
[27] Kilic G. Using advanced NDT for historic buildings: Towards an integrated multidisciplinary health assessment strategy. J Cult Herit 2015;16(4):526–35.
[28] Tinsley-Marshall P., Downey H., Adum G., Al-Fulaij N., Bourn N. A.D., Brotherton P. N.M., Frick W. F., Hancock M. H., Hellon J., Hudson M. A., Kortland K., Mastro K., McNicol C. M., McPherson T., Mickleburgh S., Moss J. F., Nichols C. P., O'Brien D., Ockendon N., Paterson S., Parks D., Pimm S. L., Schofield H., Simkins A. T., Watuwa J., Wormald K., Wilkinson J., Wilson J.D., Sutherland W. J., Funding and delivering the routine testing of management interventions to improve conservation effectiveness, Journal for Nature Conservation, Volume 67, 2022, 126184, ISSN 1617-1381, https://doi.org/10.1016/j.jnc.2022.126184.
[29] Alani AM, Aboutalebi M, Kilic G. Integrated health assessment strategy using NDT for reinforced concrete bridges. NDT and E Int 2014;61:80–94. https://doi.org/10.1016/j.ndteint.2013.10.001. ISSN 0963–8695,.
[30] Van Juijk Ko J.M.J., Haak A.M., Ritsema I.L., Reduction of equivalence in layer-model interpretation by combination of electrical resistivity soundings and electromagnetic conductivity measurements; some case histories in groundwater survey, Journal of African Earth Sciences (1983), Volume 6, Issue 3, 1987, Pages 379-384, ISSN 0731-7247, https://doi.org/10.1016/0899-5362(87)90080-7.
[31] Saberi S., Stockinger M., Stoeckl C., Buchmayr B., Weiss H., Afsharnia R., Hartl K., A new development of four-point method to measure the electrical resistivity in situ during plastic deformation, Measurement, Volume 180, 2021, 109547, ISSN 0263-2241, https://doi.org/10.1016/j.measurement.2021.109547.
[32] Tronicke J, Blindow N, Groß R, Lange MA. Joint application of surface electrical resistivity- and GPR-measurements for groundwater exploration on the island of Spiekeroog—northern Germany. J Hydrol 1999;223(1-2):44–53.
[33] Cavalcanti MM, Rocha MP, Blum MLB, Borges WR. The forensic geophysical controlled research site of the University of Brasilia, Brazil: Results from methods GPR and electrical resistivity tomography. Forensic Sci Int 2018;293:101.e1–101.e21. https://doi.org/10.1016/j.forsciint.2018.09.033. ISSN 0379–0738,.
[34] Loureiro A. M. S., Paz S. P. A., Veiga M. do R., Angélica R. S., Assessment of compatibility between historic mortars and lime-METAKAOLIN restoration mortars made from amazon industrial waste, Applied Clay Science, Volume 198, 2020, 105843, ISSN 0169-1317, https://doi.org/10.1016/j.clay.2020.105843.
[35] Fusade L, Viles H, Wood C, Burns C. The effect of wood ash on the properties and durability of lime mortar for repointing damp historic buildings. Constr Build Mater 2019;212:500–13. https://doi.org/10.1016/j.conbuildmat.2019.03.326. ISSN 0950–0618,.
[36] Theodorakeas P, Ibarra-Castanedo C, Sfarra S, Avdelidis NP, Koui M, Maldague X, et al. NDT inspection of plastered mosaics by means of transient thermography and holographic interferometry. NDT and E Int 2012;47:150–6. https://doi.org/10.1016/j.ndteint.2012.01.004. ISSN 0963–8695,.
[37] Spagnolo GS, Ambrosini D, Paoletti D. An NDT electro-optic system for mosaics investigations. J Cult Herit 2003;4(4):369–76.
[38] Palaminy L. de, Daher C., Moulherat C., Development of a non-destructive methodology using ATR-FTIR and chemometrics to discriminate wild silk species in heritage collections, Spectrochimica Acta Part A: Molecular and Biomolecular Spectroscopy, Volume 270, 2022, 120788, ISSN 1386-1425, https://doi.org/10.1016/j.saa.2021.120788.
[39] Izzo F., Germinario C., Grifa C., Langella A., Mercurio M., External reflectance FTIR dataset (4000–400 cm−1) for the identification of relevant mineralogical phases forming Cultural Heritage materials, Infrared Physics & Technology, Volume 106, 2020, 103266, ISSN 1350-4495, https://doi.org/10.1016/j.infrared.2020.103266.
[40] Franquelo ML, Duran A, Herrera LK, Jimenez de Haro MC, Perez-Rodriguez JL. Comparison between micro-Raman and micro-FTIR spectroscopy techniques for the characterization of pigments from Southern Spain Cultural Heritage. J Mol Struct 2009;Volumes 924–926:404–12. https://doi.org/10.1016/j.molstruc.2008.11.041. ISSN 0022–2860,.
[41] Ferretti V, Comino E. An integrated framework to assess complex cultural and natural heritage systems with Multi-Attribute Value Theory. J Cult Herit 2015;16(5):688–97.
[42] Cutajar D, Farrugia P-S, Micallef A. An integrated approach to the study of heritage sites. J Cult Herit 2019;37:1–8.
[43] Benedetto C. D., Gautiero A., Guarino V., Allocca V., Vita P. D., Morra V., Cappelletti P., Calcaterra D., Knowledge-based model for geomaterials in the Ancient Centre of Naples (Italy): towards an integrated approach to cultural heritage, Digital Applications in Archaeology and Cultural Heritage, Volume 18, 2020, e00146, ISSN 2212-0548, https://doi.org/10.1016/j.daach.2020.e00146.
[44] Sesana E, Gagnon AS, Bonazza A, Hughes JJ. An integrated approach for assessing the vulnerability of World Heritage Sites to climate change impacts. J Cult Herit 2020;41:211–24.
[45] Zheng D, Liang Z. Heterogeneity of residents' dilemmas in supporting sustainable heritage development: An integrated segmentation approach. J Destin Mark Manag 2021;21:100635.
[46] Annibaldi V., Cucchiella F., Berardinis P. D., Gastaldi M., Rotilio M., An integrated sustainable and profitable approach of energy efficiency in heritage buildings, Journal of Cleaner Production, Volume 251, 2020, 119516, ISSN 0959-6526, https://doi.org/10.1016/j.jclepro.2019.119516.
[47] Kioussi A., Karoglou M., Labropoulos K., Bakolas A., Moropoulou A., Integrated documentation protocols enabling decision making in cultural heritage protection, Journal of Cultural Heritage, Volume 14, Issue 3, Supplement, 2013, Pages e141-e146, ISSN 1296-2074, https://doi.org/10.1016/j.culher.2013.01.007.
[48] M. Torres-González, F.J. Alejandre, V. Flores-Alés, A.I. Calero-Castillo, F.J. Blasco-López, Analysis of the state of conservation of historical plasterwork through visual inspection and non-destructive tests. The case of the upper frieze of the Toledanos Room (The Royal Alcázar of Seville, Spain), Journal of Building Engineering, Volume 40, 2021, 102314, ISSN 2352-7102, https://doi.org/10.1016/j.jobe.2021.102314.
[49] Halaçoğlu, N. K. Mübadele İle Cami, Tekke ve Türbelerden Getirilen Kültür Varlıkları. MÜBADELE GÖÇMENLERİ VE BURSA, 184 https://www.academia.edu/download/63079344/ MUBADELE_GOCMENLERI_VE_BURSA20200424-51218-1x1vmca.pdf#page=185.
[50] İnceoğlu, E. M. A. Yapilarin algilanmasinda mimari üslup rolünün kilise ve külliye üzerinden incelenmesi. Uluslararası Disiplinlerarası ve Kültürlerarası Sanat, 4(9), 109-123. https://dergipark.org.tr/en/pub/ijiia/issue/57932/831756.
[51] Malkoç, M. Numan (2011). Türkiye'de Protestanlık ve Protestan Kiliseleri. Yalın Yayıncılık. s. 150. ISBN 9757065234.
[52] Saeli M., Senff L., Tobaldi D. M., Seabra M. P., Labrincha J. A., Novel biomass fly ash-based geopolymeric mortars using lime slaker grits as aggregate for applications in construction: Influence of granulometry and binder/aggregate ratio, Construction and Building Materials, Volume 227, 2019, 116643, ISSN 0950-0618, https://doi.org/10.1016/j.conbuildmat.2019.08.024.
[53] Blaeuer C, Kueng A. Examples of microscopic analysis of historic mortars by means of polarising light microscopy of dispersions and thin sections. Mater Charact 2007;58(11-12):1199–207.
[54] Rucka M, Lachowicz J, Zielińska M. GPR investigation of the strengthening system of a historic masonry tower. J Appl Geophys 2016;131:94–102. https://doi.org/10.1016/j.jappgeo.2016.05.014. ISSN 0926–9851,.
[55] Kilic G, Eren L. Neural network based inspection of voids and karst conduits in hydro–electric power station tunnels using GPR. J Appl Geophys 2018;151:194–204. https://doi.org/10.1016/j.jappgeo.2018.02.026. ISSN 0926–9851,.
[56] Llorente-Alvarez A, Camino-Olea MS, Cabeza-Prieto A, Saez-Perez MP, Rodríguez-Esteban MA. The thermal conductivity of the masonry of handmade brick Cultural Heritage with respect to density and humidity. J Cult Herit 2022;53:212–9.

[57] İslam G., (2018). Laboratory investigation of the effects of aggregate's type, size and polishing level to skid resistance of surface coatings. 10.13140/RG.2.2.22579.53283.

[58] Witzany J, Cejka T, Zigler R. Load-Bearing Capacity Determination of Historic Masonry Structures. Adv Mat Res 2014;923:81–4. https://doi.org/10.4028/www.scientific.net/AMR.923.81.

[59] Vercher, Jose & Gil Benso, Enrique & Mas, Ángeles. (2013). Load-bearing capacity of corroded reinforced concrete joists. 10.1201/b15267-123.